United Nations Educational, Scientific and Cultural Organization
GRÓ GTP Geothermal Training Programme Under the auspices of UNESCO

GRÓ GTP, Grensásvegur 9,
IS-108 Reykjavík, Iceland

Reports 2021
Number 13

UTILIZATION OF LOW-PRESSURE GEOTHERMAL WELLS IN OLKARIA FOR FOOD DRYING: A CASE STUDY OF MACADAMIA NUTS

George Maingi
Kenya Electricity Generating Company PLC
Olkaria Geothermal Project
P.O. Box 785 - 20117
Naivasha
KENYA
gmaingi@kengen.co.ke

ABSTRACT

Drying has been used as a food preservation method since ancient times. Solar and biomass are the main energy sources for widespread drying of agricultural products. Geothermal energy has been used for food drying in some countries around the world. In Kenya, geothermal energy has been used for pyrethrum drying since 1939, albeit on a small-scale basis. Currently, a semi-commercial pilot grain dryer has been installed at the Menengai geothermal field in Nakuru-Kenya, targeting farmers in the Rift Valley who have the need for drying grains. The current study aims to study the option to commercially utilize fluids from low pressure geothermal wells in the Olkaria Geothermal Field. Currently, these wells are not being used for power generation as they cannot be connected to a condensing turbine power plant. The study is a case study on macadamia nuts which is the most expensive nut in the world. Kenya is the third biggest producer of macadamia nuts and to reduce wastage of the nuts post-harvest, drying by use of geothermal is a possible solution.

1. INTRODUCTION

1.1 Geothermal energy – direct and indirect uses

Geothermal energy is heat that is contained within the earth's crust and can be recovered for human use. The source of the heat within the earth's crust, according to Dickson and Fanelli (2004), can be attributed to the decay of isotopes present within the earth's crust, primordial energy of planetary accretions and the radiogenic heat with the latter two being attributed to the formation of the earth. Currently, utilization of this energy is limited to a few places on earth where favourable conditions occur. According to Dickson and Fanelli (2004), the main factors that determine the ease with which geothermal resources can be exploited are:

i. Fluid availability – There must exist sufficient fluid in the earth's crust i.e., in pores and fractures, to carry the heat energy to the surface during exploitation of the resource.
ii. Heat – Heat must be available near the earth's surface. Geology plays a big role in this, and therefore commercially viable geothermal resources are limited to a few places in the world.
iii. Permeability – The fluids carrying the heat to the surface must circulate and contact the hot rock and be able to flow to the surface to bring the heat up for utilization.

To identify locations where geothermal resources are easily exploitable in the world, the geothermal gradient describing the increase of temperature with depth in the earth's crust is commonly used. On average, the geothermal gradient is 2.5 – 3°C/100 m but may be lower than 1°C/100 m in young sedimentary basins and is much higher in geothermally active areas (ThinkGeoEnergy, 2021).

Geothermal energy use can be broadly categorized into direct-use applications, geothermal heat pumps and electric power generation (Britannica, 2021). Geothermal resources have been classified depending on the temperature of the resource. Table 1 from Gehringer and Loksha (2012) is one such classification.

TABLE 1: Classification of geothermal resources (Gehringer and Loksha, 2012)

Type of resource	Temperature (°C)	Use/Technology
Low - enthalpy	Less than 150	Power generation with binary power plant technology and direct uses
Medium - enthalpy	150 - 200	Power generation with binary power plants like the Organic Rankine Cycle (ORC) and the Kalina cycle
High - enthalpy	Greater than 200	Power generation with conventional steam, flash, double flash or dry steam technology

1.2 Kenya - economy and geothermal energy

Kenya has an area size of 580,876.3 km^2 and by 2019 the population was 47,564,296 (KNBS, 2019). The majority of Kenyans practice agriculture with the sector employing 40% of the general population and 70% of the rural population, making it the backbone of the economy (KNBS, 2019). According to USAID (2021), agriculture contributes approximately 33% of the Gross Domestic Product (GDP). Manufacturing contributes 8.5% to the GDP (President's Delivery Unit, 2021) with the biggest sources of energy being industrial diesel oil (IDO), heavy fuel oil (HFO) and wood pulp (Njuguna, 2019). Global warming because of environmental pollution and the high cost of fossil fuels are becoming a major concern for a growing economy like Kenya. In the Kenyan government development agenda, contribution of GDP from manufacturing is projected to increase to 15% and one of the contributors is local value addition from nuts (PDU, 2021). The use of geothermal heat as an alternative to fossil fuels and biomass is of great importance to substitute the current energy requirement in the whole sector.

Kenya is the leading country in Africa in terms of geothermal utilization and ranks number eight (8) globally. Over the past six years, Kenya has added 218 MWe from geothermal resources to its grid, bringing the total installed capacity to 862.5 MWe (Omenda et al., 2020). The share of geothermal energy was about 30% of the total installed electricity in Kenya by June 2020 and represented about 47% of the electricity generated in the same period (Kenya Power, 2021).

1.3 Olkaria Geothermal Field - low-pressure wells

The eastern branch of the East African Rift System (EARS) which extends from the Afro Arabian rift in the Red Sea in the north to Mozambique in the southern part of Africa is geothermally active (Figure 1). The Olkaria Geothermal Field is the main producing field in Kenya. The field has been heavily drilled and is currently producing around 862.5 MWe, with plans for an additional 223.3 MWe (Omenda et al., 2020). The installed power plants in Olkaria and the average pressure at the turbine interphase are

shown in Table 2.

FIGURE 1: A simple geological map of Kenya with the main geothermal areas shown (Mwangi and Mburu, 2005)

TABLE 2: KenGen's power plants and the turbine interface pressures (KenGen, 2021a)

No	Plant	Average Interphase Pressure (bars)
1	Olkaria I	4.8
2	Olkaria I Additional Units	4.845
3	Olkaria II	5.05
4	Olkaria IV	5.71
5	Olkaria V	10.075
6	Wellhead Units	10.8 to 14.1

As shown in Table 2 above, all wells being used by KenGen in Olkaria for power production need to be above 5 bars. After separation, the hot brine from these wells is currently being reinjected. There are plans to introduce binary plants to extract more energy from the hot separated brine before reinjection. There is however a resource that is not being utilized in Olkaria. There are wells which are not able to sustain the pressures required by the separators and are therefore not suitable for power generation using condensing turbines. Some of these wells with their additional data are shown in Table 3.

TABLE 3: KenGen's 'Low Pressure Wells' while discharging via a 5" lip pipe (KenGen, 2021b)

No	Well No.	Well Pressure (bar (a))	Total mass (t/hr)	Enthalpy (kJ/kg)	Water (t/hr)	Steam (t/hr)
1	OW-906	4.9	68.5	954	52.3	10.2
2	OW-917A	4.9	32.4	1681	14.2	16
3	OW-49A	1.69	30.6	1556	15.2	13.2
4	OW-205	4.5	71.8	878	57.2	8.1
5	OW-205A	5.2	75	1005	55.5	13
6	OW-803A	6.1	94.7	992	70.7	15.8
7	OW-803	4.4	55.9	1124.3	38.4	12.8

The main objective of this study is to design a pilot dryer that will be used to dry macadamia nuts. The fluid to power the dryer will be from one of the low-pressure geothermal wells, and the production characteristics, well location and geochemistry of the wells will be used to determine the best location for the pilot plant.

1.4 Introduction to macadamia nuts

Macadamia, whose botanical name is *Macadamia integrifolia,* is an evergreen tree, originating from the coastal rainforests of Australia (Zuza et al., 2021). The tree produces nuts that have a similar appearance as small green limes. The husk is green in colour, but the pay product is a white nut inside a hard seed coat (shell) (Tompson et al., 2009). Figure 2 shows the macadamia nut.

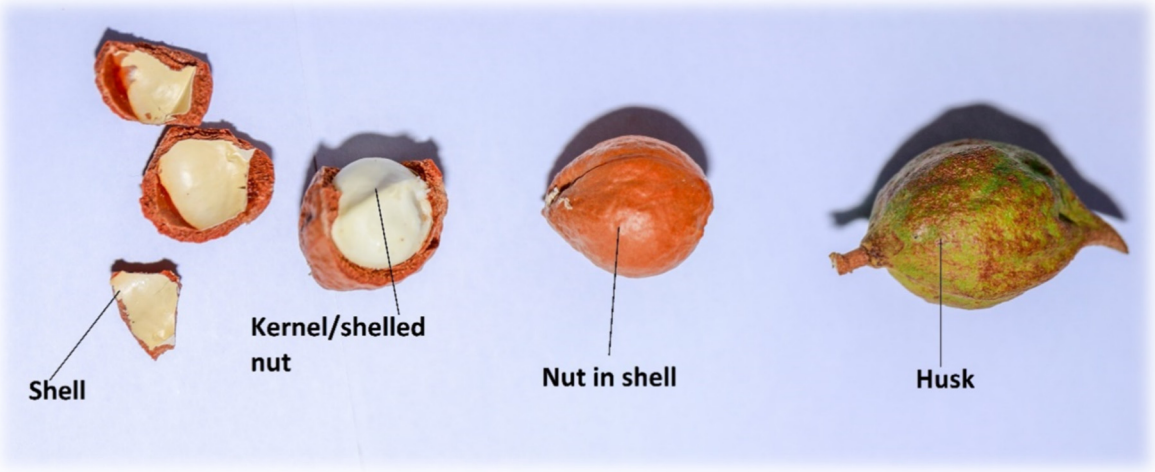

FIGURE 2: Macadamia nut (Hyzoh Visuals - Kenya, 2021)

Macadamia's buttery flavour and velvety-soft crunch taste make them a delicacy amongst consumers. Apart from the great taste, macadamias nutritional composition of monosaturated fats, fibre, magnesium, copper, manganese, thiamine, vitamins B6, niacin, iron, phosphorus, potassium, and selenium resulted in them being regarded as a super food (INC, 2018; Maxim International, 2019).

The annual global production of macadamia kernels has been on an upward trend for the last decade and Kenya has risen to be the third biggest producer in the world (Figure 3).

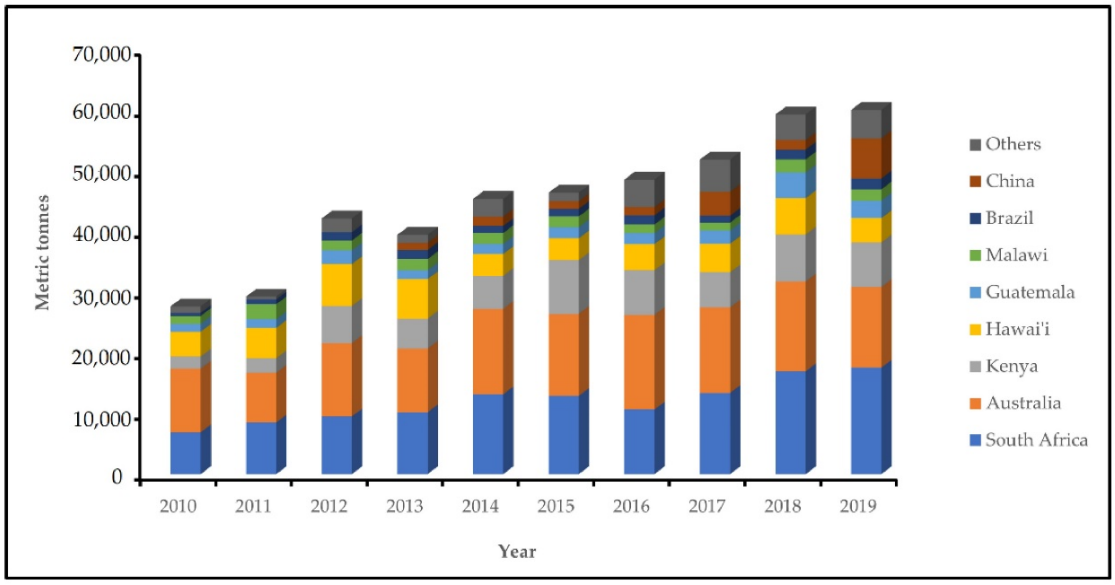

FIGURE 3: Global macadamia kernel production (Zuza et al., 2021)

In Kenya, the tree is grown in coffee and tea growing zones by both small-scale and large-scale farmers (Njuguna, 2021). Due to their popularity and high demand on the world market, macadamia farming and processing is a lucrative industry whose production costs can be lowered to decrease production cost.

Drying of macadamia nuts is one of the most important stages in processing the product for the consumer market. It is imperative that the drying processes commences as soon as possible after harvesting. This prevents hydrolytic rancidity inside the nuts or mould on the nuts from developing. Nuts which have been dried to a moisture content of 1.5% dry basis (d.b.) are storable for a period of 12 months without much loss of the product quality (Mason and Willis, 2000 in Silva et al., 2005).

Macadamia has become a key foreign exchange earner for Kenya in the recent years. An increase in production is expected as more farmers have been growing the plant and with nut in shell (NIS) production is expected to reach 60,000 tons by the year 2022 (Quiroz et al., 2019). There is therefore demand for better and more efficient processes as the harvest will get bigger in the future. Macadamia has been labelled the most expensive nut in the world and is not only consumed as a snack, but is also finding use in baking and confectionery, cooking oil, cosmetic and beverage industries (INC, 2018).

2. THIN LAYER DRYING OF MACADAMIA NUTS

2.1 Introduction

Since ancient times, drying has been widely used as a method of grain, fruit, and vegetable preservation. The objective of drying is to reduce the moisture content in the produce, and therewith increase its lifetime by limiting enzymatic and oxidative degradation. As a result of this, drying reduces crop losses, improves quality of the products, and facilitates cost-effective transportation, handling, and storage requirements (Ertekin and Firat, 2017).

Thin layer drying is the method mostly used to estimate the drying characteristics of agricultural

products (Phusampao, 2014). The drying process mechanism does not only involve simultaneous transfer of heat and mass within the material but also between the surface of the material and the surrounding media. The mechanisms describing the transport phenomena as described by Sabarez (2018) is shown in Figure 4.

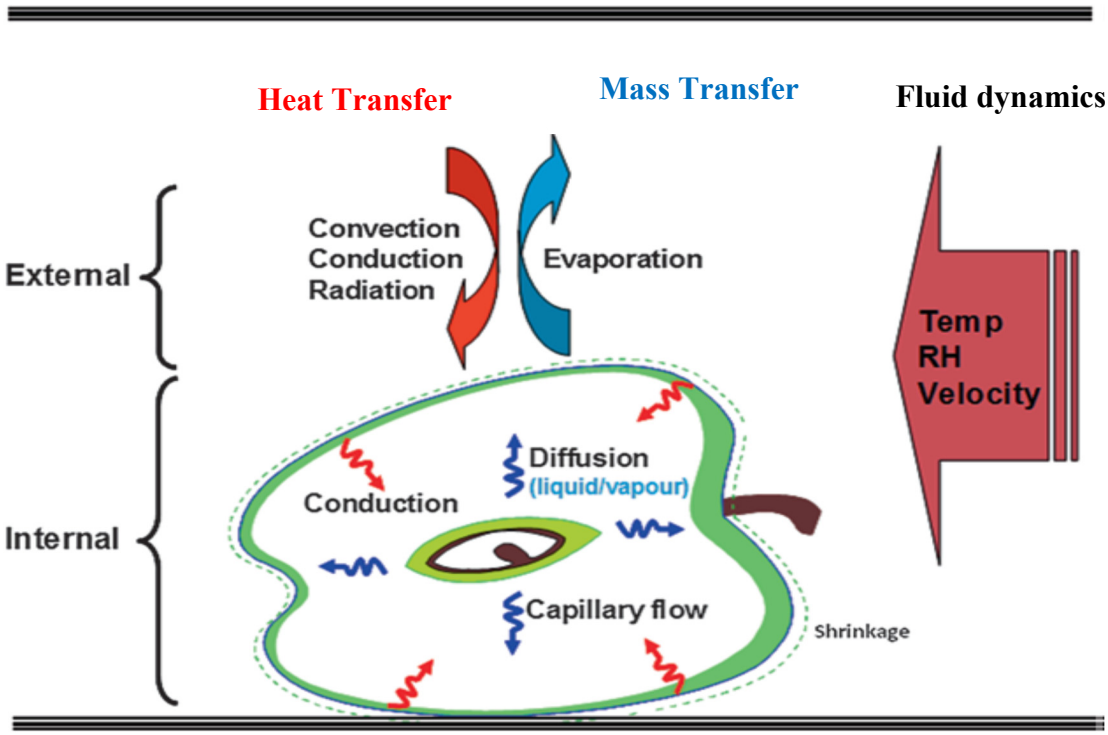

FIGURE 4: Conceptual representation of transport phenomena in solid food drying (Sabarez, 2018)

The equations and their relations with other properties that govern thin layer drying are shown in Figure 5 (modified from Ertekin and Firat, 2017).

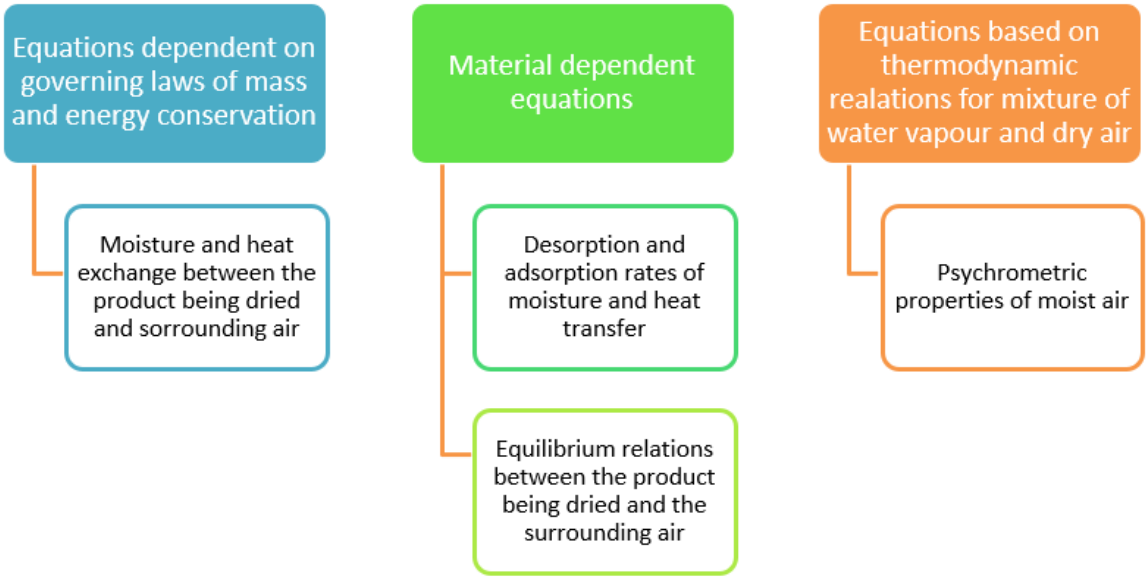

FIGURE 5: Equations and their relations in layer drying models. Modified from (Ertekin and Firat, 2017)

The term “thin layer” has been broadly used in various drying models. According to Ertekin and Firat (2017), “thin layer” can be applied to a model or a process that satisfies the following:

i. That the product being dried is a single kernel freely suspended in the drying air, or that the product is in a single layer of grain kernels.
ii. Or that if the grain kernels are in multiple layers, the temperature and relative humidity of the drying air can be in the same thermodynamic state at the time of drying. This is the state that is used in the drying process calculations.

Consequently, the conclusion drawn from this is:

i. A mathematical model of drying a single kernel of grain can be extended to drying of grains in a thin layer.
ii. The thickness of this thin layer may vary in air velocity, relative humidity, and the temperature of the drying air.

2.2 Evaluation of thin layer drying models in drying of macadamia nuts

Thin layer drying equations and models are the basis of all drying simulations. They describe the relationship between the moisture exchange of a thin layer of the drying product with its surrounding air.

According to Ertekin and Firat (2017), Fick's second law of diffusion can be used to express the mechanism of biological product drying, given the following generalizations:

i. The kernel of macadamia nuts can be represented by a sphere and the shell by a slab.
ii. Uniform initial moisture content distribution is assumed.
iii. Only one dimension moisture diffusion takes place.
iv. No shrinkage takes place during the drying process.
v. There is negligible external resistance to air and mass flow.
vi. The effective moisture diffusion coefficient is constant throughout the drying period.

Fick's second law of diffusion applied to describe a moisture diffusion process is shown in Equation 1 below (Ertekin and Firat, 2017):

$$\frac{\partial m}{\partial t} = D_{eff}\, \nabla^2\, m \tag{1}$$

where m = local moisture content on a dry basis (d.b);
t = time in seconds; and
D_{eff} = moisture diffusivity in m^2s^{-1}.

Thin layer drying models developed from data obtained from drying macadamia nuts have been expressed in the form of moisture content ratio in the samples as shown in Equation 2 (Phusampao, 2014):

$$MR = \frac{M_t - M_e}{M_0 - M_e} \tag{2}$$

where MR = dimensionless moisture ratio or moisture content;
M_t = Moisture content at any given time;
M_e = Equilibrium moisture content of air at the prevailing conditions; and
M_o = Original moisture content of the sample at the beginning of drying.

Tumba (2018) expresses moisture content M_t at any time as kg H_2O / kg of dry mass in the form of Equation 3 below:

$$M_t = \frac{m_w}{m_{db}} = \frac{m_t - m_{db}}{m_{db}} \quad (3)$$

where M_t = Moisture content at any given time *t*;
m_w = Mass of water in the sample at the given time *t*;
m_{db} = Mass of the dried sample; and
m_t = Mass of the sample being dried at the given time *t*.

Phusampao (2014) was able to show a correlation between predicted moisture content (%, d.b.) and observed moisture content in an experiment they conducted. The experiment was repeated nine time, and then the data was analysed and plotted. The experiments were conducted at relative humidity values of 10%, 20% and 30%, and temperatures of 40°C, 50°C and 60°C. Figure 6 below shows the results from the experiments.

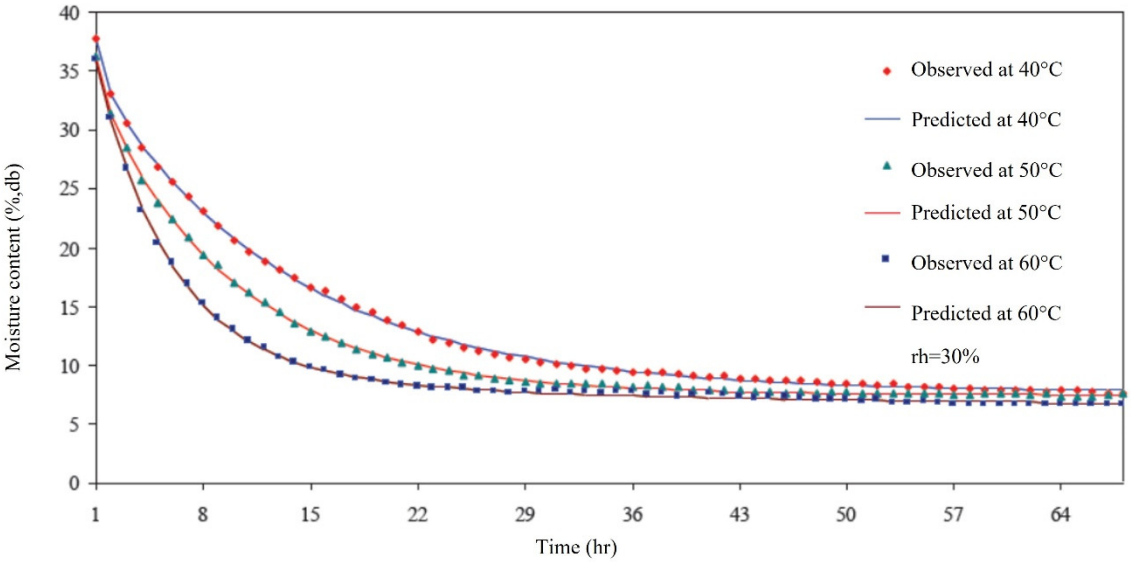

FIGURE 6: Predicted and observed moisture content of in-shell macadamia nuts using modified Henderson and Pabis model at the temperatures of 40°C, 50°C and 60°C and relative humidity of 30% (modified from Phusampao, 2014)

Njuguna (2021) reports that the drying of two varieties of macadamia nuts using different drying methods can be modelled using both Approximation of Diffusion and Modified Henderson and Pabis models. He conducted experiments on varieties KRG-15 and MRG-20 of macadamia nuts in Thika, Kenya. In his experiments, he used oven drying at 50 – 60°C, a solar tent dryer, solar tent then microwaves and finally solar tent and oven at 60°C. Other researchers have reported that thin layer modelling of macadamia nuts drying is sufficiently accurate (Toyoda et al., 1991; Wang et al., 2013; Tumba, 2018; Ertekin and Firat, 2017). Therefore, it is sufficient to model drying of macadamia using a thin layer model.

2.3 Chosen sorption isotherm for design

Moisture sorption isotherms in food preservation describe the relationship between the equilibrium moisture content of the product and the relative humidity of air surrounding the product at a constant

temperature. In macadamia nuts storage, the isotherms determine the packaging and storage of the nuts (Phusampao, 2014). The isotherm shows how water activity a_w changes as water is adsorbed into or desorbed from a product during the drying process, and especially the final moisture content is dependent on it. Water activity is defined as the ratio of water vapour pressure in the system, macadamia nuts in this case, and the pure water vapour pressure at a constant pressure and temperature (Andrade et al., 2011).

Phusampao (2014), after conducting experiments and fitting the data on five isotherms for macadamia nuts, concluded that the Modified Oswin model was best suited for predicting the water activity in dried macadamia nuts. Furthermore, they concluded that the equilibrium moisture content decreased with an increase in drying temperature and increased with an increase of relative humidity of the surrounding air.

2.4 Diffusivities of the shell and kernel of macadamia nuts

Fick's second law can be used to express the mechanism of macadamia drying, given the following generalizations (Phusampao, 2014):

i. The kernel of macadamia nuts can be represented by a sphere and the shell by a slab.
ii. Uniform initial moisture content distribution is assumed.
iii. Only one dimension moisture diffusion takes place.
iv. No shrinkage takes place during the drying process.
v. There is negligible external resistance to air and mass flow.
vi. The effective moisture diffusion coefficient is constant throughout the drying period

Toyoda et al. (1991), concluded that macadamia nuts can be represented as a sphere with a high degree of accuracy. For a sphere, the analytical solution of Equations 1 and 2 is given as Equation 4 below:

$$\frac{M_t - M_e}{M_0 - M_e} = \frac{6}{\pi^2}\sum_{n=1}^{\infty}\frac{1}{n^2}\, exp\left(-n^2\pi^2\frac{D_{eff}\, t}{r^2}\right) \tag{4}$$

where D_{eff} = moisture diffusivity in m^2s^{-1};
r = effective radius of the nuts; and
n = number of terms of the Fourier series.

Experimental models on drying of nuts have been fitted to the expanded form of equation 4 above, and the first three terms have been found to give an accurate result. This solution is generally known as the Modified Henderson Pabis model where the first term was found to explain the later drying stages, the second term approximates the behaviour in intermediate drying stages and the third term approximates the beginning of the drying process. The general form of the equation is shown as Equation 5 here below:

$$\frac{M_t - M_e}{M_0 - M_e} = a\, e^{-k_0 t} + b\, e^{-k_1 t} + c\, e^{-k_2 t} \tag{5}$$

The drying parameters *a, b, c, k_0, k_1 and k_2* are process specific and are determined by different factors like the initial moisture content of the product, the drying temperature used, relative humidity inside the dryer and the duration of drying (Phusampao, 2014).

Based on the foregoing discussions, it is safe to model the drying of nut in shell macadamia as a thin layer process, as different authors have conducted experiments and proven that the models work. The starting conditions vary from one author to the next, and therefore, the drying parameters are never the same. These should be found out on a case-to-case basis, and equation (5) can be used to estimate the drying rate, drying time, or final moisture content.

3. GEOTHERMAL WELLS ANALYSIS

3.1 Introduction

A geothermal well is specially made to tap and conduct hot fluids from the subsurface to the surface for exploitation of energy. The fluids can also be used as a source of valuable minerals. This is because the geothermal fluids interact with the host rocks as they percolate through the hot rock bodies, and therefore, get saturated with different minerals (Bloomquist, 2006).

A typical geothermal well has five different sections as shown in Figure 7. After drilling, the upper parts of the well are cemented to anchor the well firmly into the ground as well as provide isolation from upper surface water and formation, thereby preventing contamination of the shallower, colder fluids. The production section is made up of perforated liners which allow the hot fluids to flow up the well (Ingason, 2021).

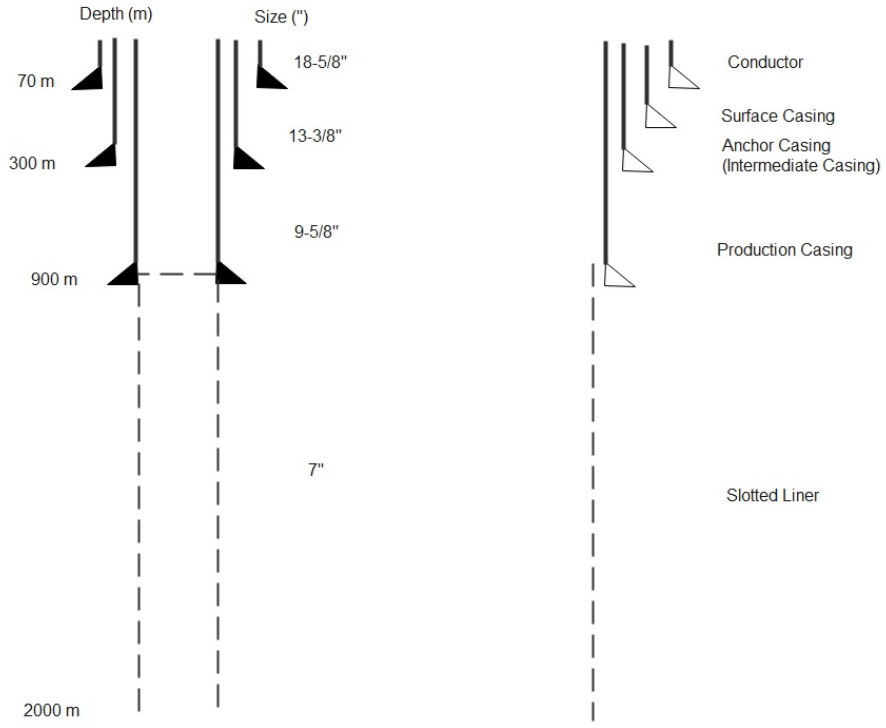

FIGURE 7: Typical Geothermal well profile (modified from Ingason, 2021)

Geothermal wells have not only made it possible to extract more energy from the reservoirs because of increased flow, but they also provide access to deep reservoirs and data which can be used to model the reservoirs to improve our understanding of them (Axelsson, 2013).

In Olkaria, the geothermal resource has mainly been used for electrical power production. The installed capacity for electricity production is about 865 MWe while 30 MWt is being used for flower farming at Oserian and recreational purposes at the Olkaria geothermal spa (Mangi, 2019). To allow for prudent

management of the field exploration and exploitation, the Olkaria Geothermal Field is divided into seven segments as shown in Figure 8.

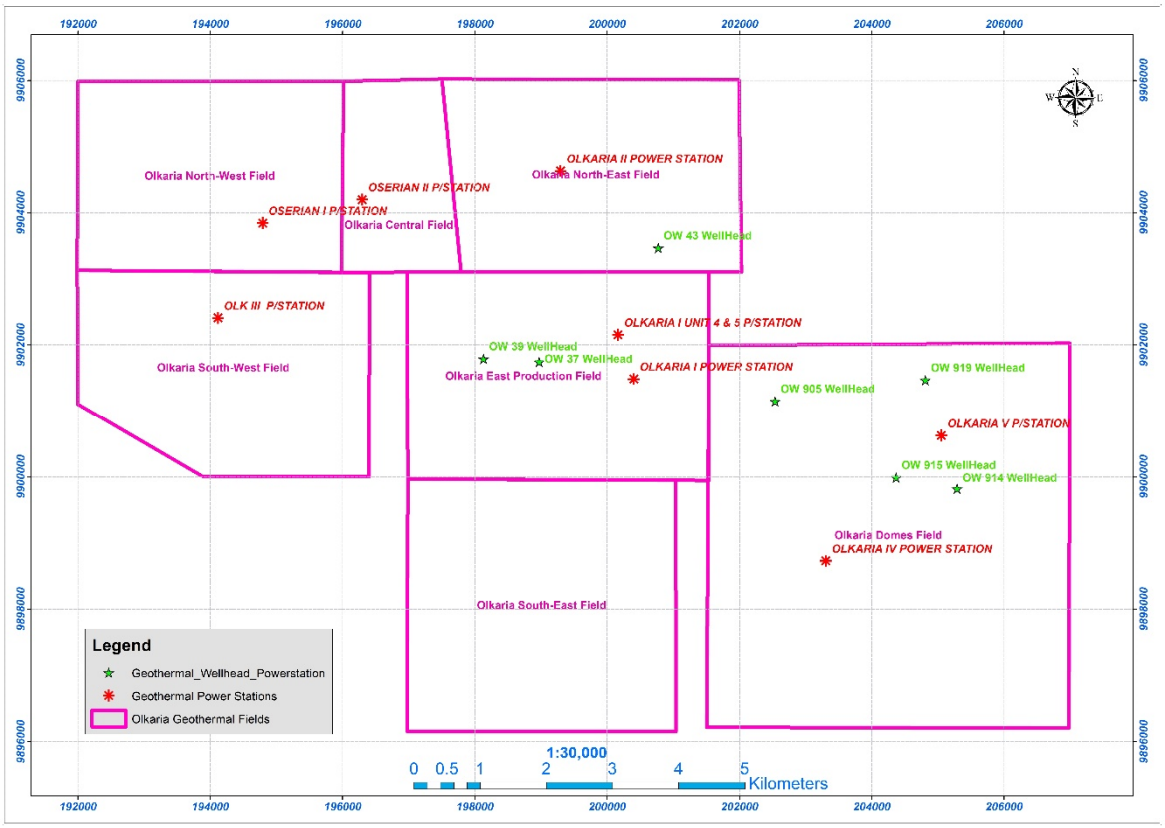

FIGURE 8: Sectors in Olkaria Geothermal Field (KenGen, 2021c)

Discharge testing shows that not all wells have the required characteristics to be used in condensing turbines for power generation. KenGen has got a number of these wells which do not produce at the required parameters. These wells will be discussed in more detail below.

3.2 Fluid flow and enthalpies

Each geothermal well is usually connected to the geothermal reservoir from where it draws its fluids through feed zones. The feed zones are either permeable aquifers or open fractures in the bedrock, and a well can be fed by one or more feed zones.

For all geothermal wells, the amount of energy that can be extracted from the fluids is determined by the well's enthalpy. Enthalpy is defined as the energy content per unit mass of the fluid and is measured in units of kJ/kg (Gao et al., 2020). High enthalpy wells have higher temperatures, can self-discharge and generally have higher reservoir pressures. As a minimum design pressure for a power plant is determined, some wells drilled in a particular field may not have the right characteristics to be connected to a power plant. In Olkaria, the current power plants require a minimum of 5 bars at the turbine interface (Table 2). This means that the wells that have lower pressures are not suitable for this form of utilization. Some of the tested wells have good characteristics for direct utilization in drying. The flow is enough for commercial utilization as a source of energy for the drying industry. These wells are mostly liquid dominated and as flow up the well bore is isenthalpic, the enthalpy conditions present in the major feed zones can be assumed to be the conditions at the surface (Guðni Axelsson, director of GRÓ GTP, personal communication, 28 October 2021).

3.3 Geochemistry

Geochemical composition of geothermal fluids is the main contributor to technical problems in geothermal utilization. This is because the geothermal fluids contain considerable amounts of minerals and gases which have a high potential to cause corrosion and scaling. This can happen in both the wells and in surface installations through which the geothermal fluids flow (Gunnlaugsson et al, 2014).

Various minerals present in geothermal brines have the potential to corrode different parts of the dryer. An analysis of the well will be carried out to mitigate corrosion by choosing favourable materials and operating conditions. Some of the minerals present in geothermal brines and their effect are shown in Table 4 (Gunnlaugsson et al, 2014).

TABLE 4: Corrosive species in geothermal fluids and possible mitigations

Species	Effect and mitigation
Hydrogen ion	Corrosion rates of most materials increase with decrease in pH. Geothermal fluids vary in pH from as low as 2 to as high as 12. As low pH waters corrode carbon steel and causes corrosion cracking in stainless steels, mild steel is a suitable substitute for vessels and pipes that are in contact with geothermal fluids.
Chloride	Both pitting corrosion and uniform corrosion on metal surfaces is possible where chloride ions are present. To prevent this, oxygen should be excluded where chloride levels are high.
Hydrogen Sulphide	This gas attacks copper and copper alloys and causes stress cracking in high strength steels. Mild steels should be used if possible.
Carbon dioxide	This gas is a mild oxidizing agent that causes increased corrosion of plain carbon steels. Stainless steels can be considered as a substitute.
Ammonia	Mild steels and copper-based alloys are affected by ammonia and should be substituted in places where high levels of ammonia are present.
Oxygen	Although oxygen is not usually present in geothermal fluids, intrusion of atmospheric oxygen should be avoided. Injection of hydrogen sulphide into the geothermal fluid rich in oxygen will cause a reaction and therefore mitigate corrosive effects of oxygen.

Scaling is another geochemistry problem, and several types of scales are observed in geothermal installations. The most common scales are silica (SiO_2) and calcite ($CaCO_3$), and accumulation of them can clog pipes and inhibit efficient heat transfer in the heat exchangers. Silica scaling is preventable by operating the installation above the solubility level of amorphous silica (Gunnlaugsson et al, 2014).

To find safe operating conditions for the production well, surface equipment and for the reinjection well, a silica scaling assessment was carried out. The geochemical composition of the fluids from the low-pressure well was analysed, and both the silica and quartz scaling curves plotted. The curve for the chosen site is shown in Figure 9. The reason for choosing this site is further discussed in section 4.6.1 of this report.

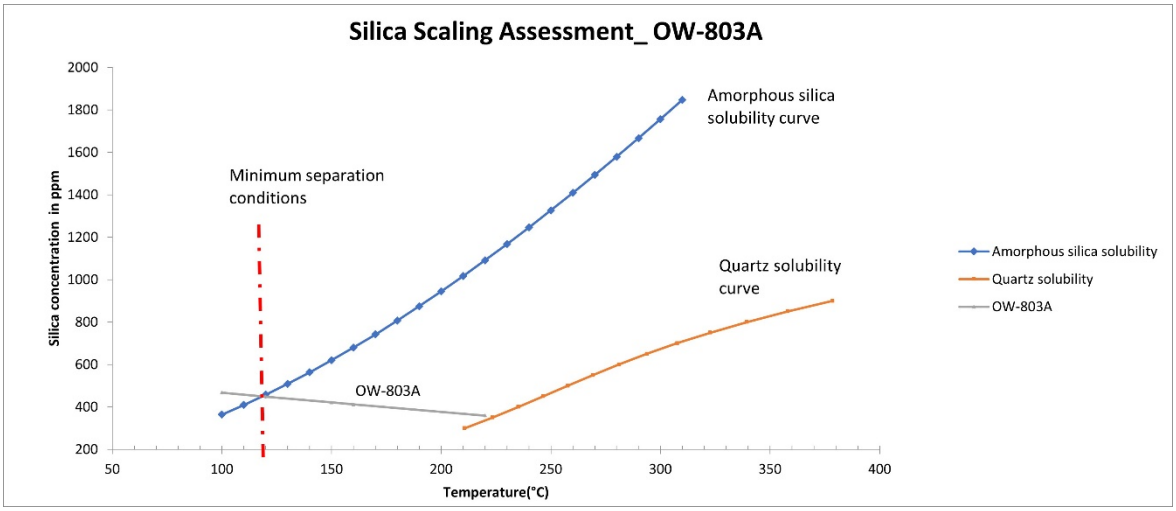

FIGURE 9: Silica and quartz solubility curves for OW-803A, showing minimum operating temperature of 120°C (KenGen, 2021d)

4. OPTIMIZATION OF DESIGN CONSIDERATIONS FOR A PILOT PLANT

4.1 Types of dryers

Since drying has been carried out for a long time in almost all parts of the world, over 500 types of dryers have been reported in technical publications to exist, with about 100 different types available commercially. The large number of dryer designs is not only determined by geographical location of where the dryers are constructed but is also dependent on physical attributes of the product being dried, operating parameters such as temperature and pressure, how the heat is supplied into the dryer and the quality required of the dried product (Mujumdar and Law, 2010).

While other industries like paper making, wood and waste management utilize drying in their processes, food and agriculture remain the most dominant users of this technology as drying plays a critical factor in the quality of their products (Mujumdar and Wu, 2010). Most convectional dryers use hot air as a medium to carry away the water vapour, they are easier and simpler to operate, than other drying methods (e.g. contact dryers, vacuum dryers,) and have a lower capital cost. Their major drawback is reduced efficiency (Sabarez, 2018). Table 5 summarises a general classification of convectional dryers in use for food drying.

A general principle of dryers and dryer use is that a type of dryer which is successfully used for one product can give a very different outcome if tried on another product. Consequently, the same type of material may need to be dried in different ways in a different dryer. Currently, the main challenge in the drying of food materials is achieving a process that rapidly removes the moisture from the material, with better retention of quality of the product, without damaging the environment, at the lowest capital and operating costs (Sabarez, 2018). Geothermal energy is environment friendly and operating costs are low.

TABLE 5: General classification of convectional thermal food dryers (Adapted from Sabarez, 2018)

Classification	**Types of dryers (general characteristics and applications)**
Composition of feed material	• Particles
	• Slurry/paste/sludge
	• Liquid suspension
Processing mode	• Batch
	• Continuous
Heat transfer mode	• Convection
	• Conduction
	• Electromagnetic (RF, ohmic, infrared, microwave)
Sources of Energy	• Electricity
	• Gas (natural/LPG)
	• Solar/wind
	• Biomass
	• Geothermal
Operation Mode	• Cyclic
	• Intermittent
	• Continuous
Temperature of the product	• Above freezing point
	• Below freezing point
Process operation pressure	• Atmospheric
	• Vacuum
	• High pressure

Due to globalization, competitiveness has increased in all sectors and consumers are demanding higher quality products that are produced in a sustainable manner. Energy efficiency, cost effectiveness and product quality are factors driving research and development in the food drying industry. As drying uses vast amounts of energy, its environmental impact has become a key factor for the industry in the 21st century.

4.2 Fixed bed dryer

Fixed bed dryers have rectangular bins with plenum chambers underneath (Figure 10). The product to be dried is laid on a perforated surface and the drying air is forced from below to dry the product as it rises in the column. The air is blown by an electric fan and passes over a heat exchanger that is fuelled by fossil fuels or biomass. This dryer is cheap to install and maintain but has the setback of having a moisture gradient as the product in the entry dries quicker than the product at the exit of the drying air. This can be reduced by redesigning the air flow such that it can be reversed during the drying process (IRRI, 2021).

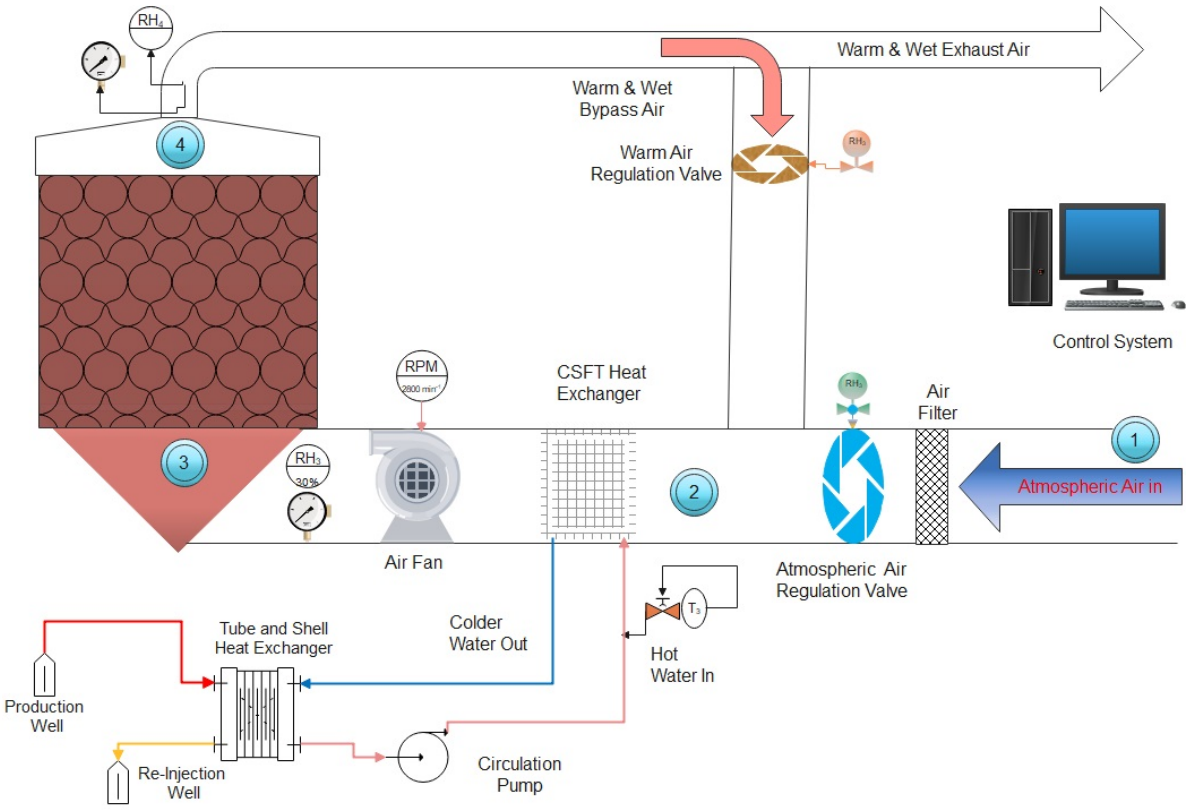

FIGURE 10: Fixed bed dryer with the four properties reference points

4.3 Mass balance and the drying process

The law of conservation of mass states that during a chemical or physical change, the total mass of the resulting products remains equal to the mass of the initial reactants at the beginning of the process. In a drying process, this law of conservation of mass and law of conservation of energy, which states that energy cannot be created nor destroyed, but can only be transformed to a different form govern the processes taking place inside the dryer. The two equations governing the drying process are shown in Figure 11.

FIGURE 11: Material and energy balance equations

The heat and mass transfer involved in the geothermal drying process was described by Arason (2018) as shown in Figure 12.

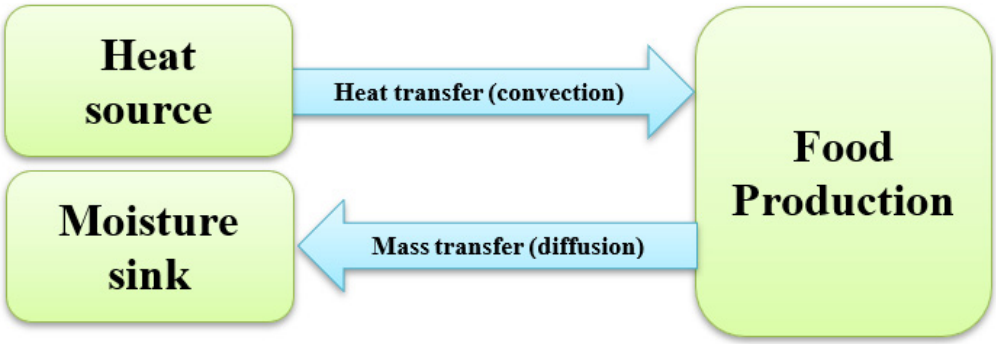

FIGURE 12: Heat and mass transfer in a drying process (modified from Arason, 2018)

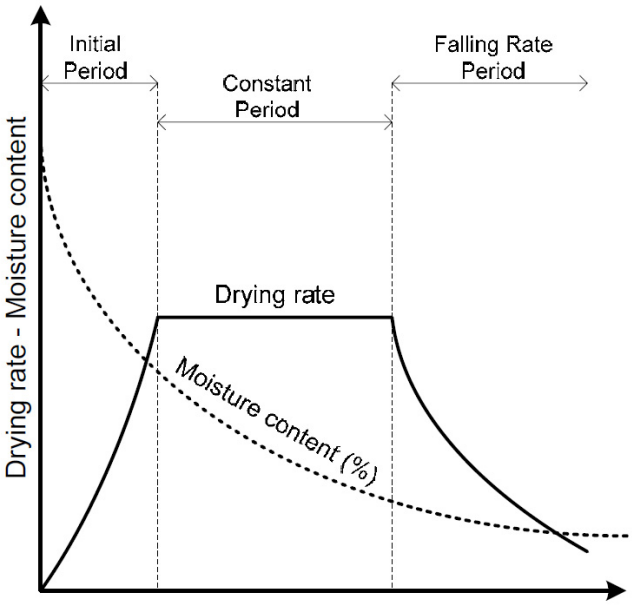

FIGURE 13: Typical drying curve behaviour showing the different phases (Tesha, 2006)

Drying typically includes three different phases, with each product and material having a different curve drying curve that describes its drying behaviour. The three phases can be represented as in Figure 13 below (Tesha, 2006), and are explained further here:

- *Initial period*: This phase occurs after the product has been loaded into the dryer. As the temperature in the dryer rises with admission of hot air, the temperature of the product rises, too. The final product temperature is close to the drying air temperature. The product's drying rate increases during this period.
- *Constant period*: During this phase, the drying rate has peaked and stabilizes. The rate of water evaporation is equal to the rate of water particle movement from inside the product to the outside. Drying rate remains high without any further change in temperature.
- *Falling rate period:* Within this phase, much water has diffused from the product and the movement of water particles from the centre of the product to the surface slows down. The drying rate therefore decreases until there is no more water evaporation, from where the temperature of the product in the dryer starts to rise.

4.4 Mass flow during drying of macadamia nuts

Drying mass flow is divided into two distinct phases, primary drying and secondary drying (Arason, 2021). For the case of macadamia nuts, the mass flow analysis is done assuming a sample of raw material weighing 100 kg, with an initial moisture of 20%. The drying is carried out in 2 stages. The primary drying reduces the water content to about 12% using a drying temperature of 40°C (Figure 14). Secondary drying reduces the moisture content to between 1.5% - 2%, and this is done at a temperature of 50°C (Figure 15). This method of drying has been reported to give the best quality in terms of colour and lipid quality (Warangkana, 2012). Final drying at 50°C was found to produce grade one macadamia nuts for the two varieties grown in Kenya, KRG-15 and MRG-20 (Njuguna, 2021).

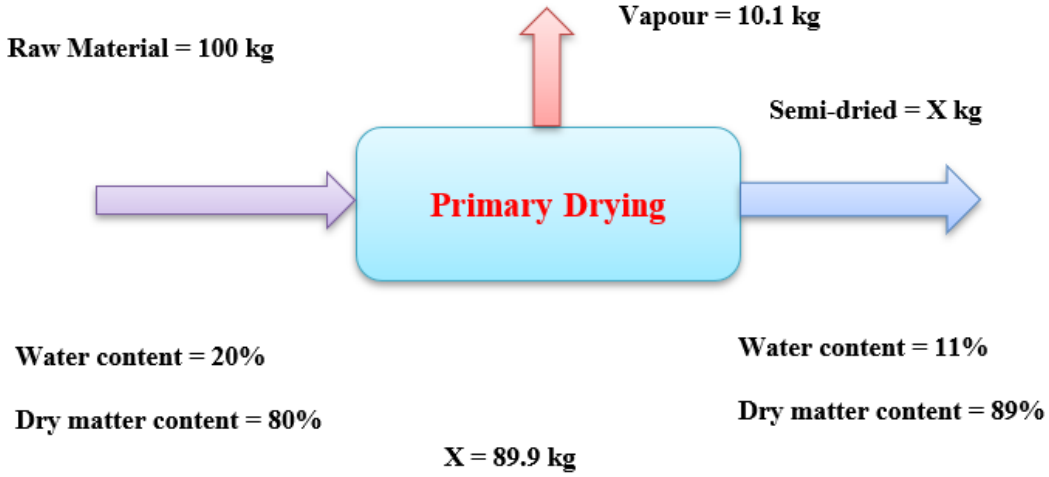

FIGURE 14: Primary drying mass balance – An input of 100 kg of 20% moisture content material gives 89.9 kg of semi dried material (Arason, 2021)

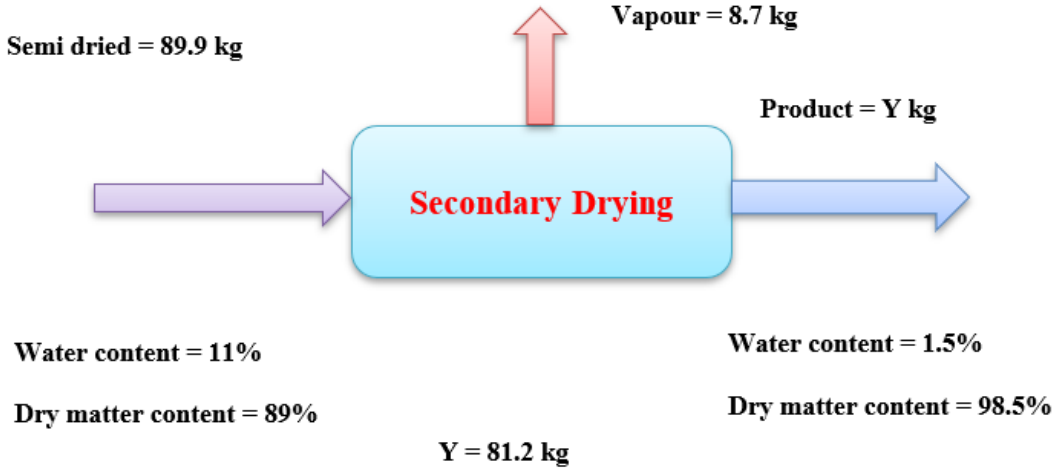

FIGURE 15: Secondary drying mass balance – An input of 89.9 kg of 11% moisture content semi-dried material gives 81.2 kg of product (Arason, 2021)

Table 6 summarizes the masses at the start, during drying and at the end of the drying process. Primary drying removes 53.7% of the moisture while secondary drying removes 46.3% of the water content from the raw material.

TABLE 6: Mass balances during the drying process

Product Type	**Total Mass at Start**	**Moisture Mass**		**Dry Matter Mass**		**Evaporated Vapor**		**Total Mass at end**
Parameters	**kg**	**Kg**	**%**	**kg**	**%**	**kg**	**%**	**Kg**
Raw material	100	20	20	80	80	0	0	100
Primary drying	100	20	20	80	80	10.1		89.9
Secondary drying	89.9	~10	11	80	89	8.7		81.2
Product		1.2	1.5	80	98.5			81.2

The various factors that determine the drying rate of material can be classified as external and internal (Tesha, 2006).

- External factors affecting drying rate:
  i. Velocity and turbulence of drying air.
  ii. Drying air temperature.
  iii. Material surface area and thickness.
  iv. Humidity.
- Internal factors affecting the drying rate:
  i. The type of material being dried as this affects the migration of moisture to the surface by diffusion.
  ii. Capillary flow and flow due to pressure gradients as caused by gravity.
  iii. Internal vaporization of moisture.

The laws of conservation of mass under steady state, as earlier defined, will be used in the technical design.

The law of conservation of mass is restated in Equation 6 below:

$$M_{rm} = M_v + M_p \tag{6}$$

where M_{rm} = Mass of the raw material;
M_v = Mass of vapour leaving the dryer; and
M_p = Mass of dried product.

The material balance of the moisture is described in Equation 7:

$$M_{rm} * X_{rm} = M_v * X_v + M_p * X_p \tag{7}$$

where M_{rm} = Mass of the raw material;
M_v = Mass of vapour leaving the dryer;
M_p = Mass of dried product;
X_{rm} = Moisture content of the raw material (kg of water in a kg of raw material);
X_v = Moisture content of food vapour leaving the dryer (kg/kg of dry air); and
X_p = Moisture content of the dried product (kg of water in a kg of dried product).

The weight of the water vapour being evaporated per hour m(t) is defined by Equation 8:

$$m = \frac{M_v}{t} \tag{8}$$

Density of air is given by Equation 9:

$$\rho = \frac{M_a}{V_a} \tag{9}$$

where ρ = Density of air, given as 1.225 kg/m^3;
M_a = Mass of air in kg; and
V_a = Volume of air in m^3.

The product yield is given by Equation 10:

$$Yield\ (Y) = \frac{M_p}{M_{rm}} * 100\% \tag{10}$$

The terms of this equation are defined in Equation 7 above.

Thus, the amount of air flow needed for drying the product is defined by Equation 11:

$$G = \frac{\Delta M}{\Delta X} \tag{11}$$

where G = total mass of air required to dry the raw material;
ΔM = difference in mass between the raw material and final product; and
ΔX = difference in moisture content of the air entering the dryer and the air leaving the dryer.

The mass of air needed to dry the raw material per unit time *G'*, usually per hour, is defined by Equation 12:

$$G' = \frac{G}{t} = \frac{\frac{\Delta M}{\Delta X}}{t} = \frac{\frac{\Delta M}{t}}{\Delta X} \tag{12}$$

4.5 Energy balance and air flow in the dryer

Figure 10 shows a simple flow diagram of a fixed deep bed dryer.

Point (1) is the air intake from the atmosphere. This air is at atmospheric relative humidity and atmospheric temperature. At point (2), the atmospheric air is mixed with some of the exhaust air from the dryer exhaust. The conditions at this point are determined by the mixing ratios of the two air streams. This air then passes through the heat exchanger, gaining heat in the process. The air at point (3) has reached the design parameters required to dry the raw material at that reference point. During the drying process, the water content in the raw material keeps changing and the parameters of the air at point (3) need to be regulated to reflect this. The air then passes through the product drying the moisture on the surface by evaporation. The air at point (4) has the highest moisture content and is either exhausted to the atmosphere or recycled back to the dryer inlet through the bypass line. This recycling helps save energy as the air is not completely cold as it exits to the atmosphere and the high moisture content also helps regulating the moisture content at point (3) to prevent case hardening of the product due to over-drying.

From point (2) to point (3), the air is only gaining heat at a constant water ratio content. The dry bulb temperature increases during this period. From point (3) to point (4), the air is carrying away the moisture from the surface of the raw material at a constant enthalpy (Arason, 2021). The temperature difference between the drying temperature T_3 and exhausted air temperature T_4 will be constrained to 5°C with recirculation of air to maintain optimal drying in the chamber. This will ensure that maximum heat is used up in the drying process, increasing the dryer's efficiency. To prevent case hardening on the raw material, a drying humidity ratio greater than 30% is recommended (Arason, 2021). Considering the Olkaria Geothermal Field as the pilot project for the dryer, the information in Table 7 needs to be incorporated into the dryer design for the primary stage of drying.

TABLE 7: Primary drying air and dryer parameters

Parameter	**Value**	**Comment**	**Source**
Ambient Temperature (T_1)	25°C	Annual average	KenGen (2021e)
Relative Humidity (RH_1)	70%	Annual average	KenGen (2021e)
Ambient pressure (P_{amb})	101.5kPa		
Drying temperature (T_3)	40°C	Researched value	Njuguna (2021), Warangkana (2012)
Relative Humidity (RH_3)	40%	Researched value	Arason (2021)
ρ_{air} (@ T_3, RH_3 *and* P_{amb})	1.1179 kg/m^3		

Combining the Mollier Chart (Psychrometric Chart) and the data points in Table 7, we get the data points

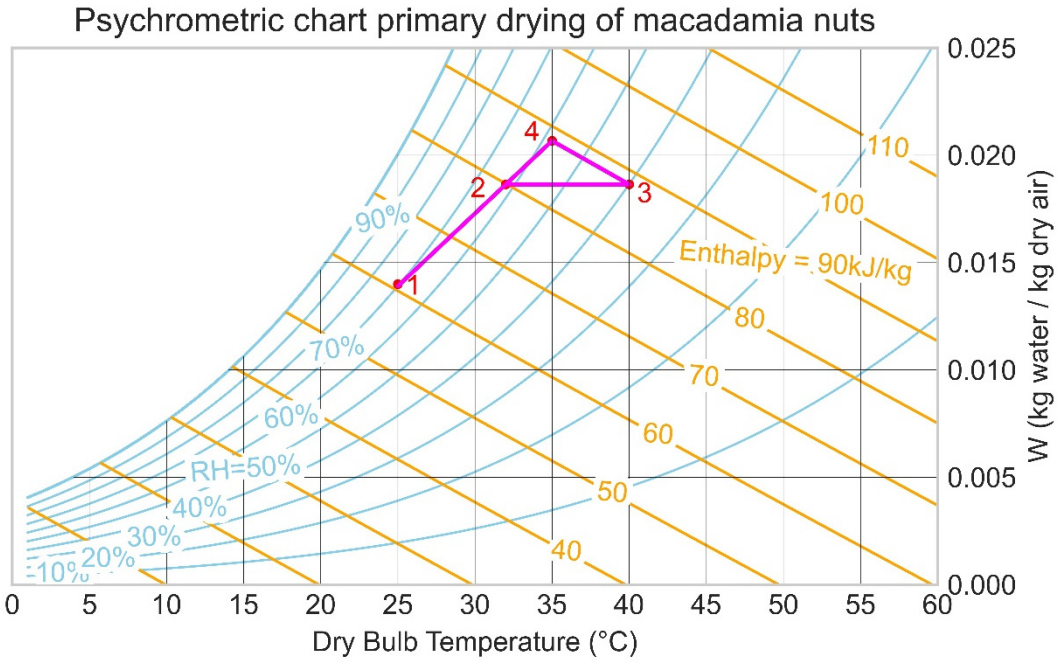

FIGURE 16: Data points plotted on Mollier chart for primary drying

plotted in Figure 16 and listed in Table 8.

The air properties in the four sections of the dryer are shown in Table 8.

TABLE 8: Properties of each dryer section in the primary drying phase at atmospheric pressure of 101.5 kPa

Point	**T (°C)**	**RH (%)**	**X (g water/kg air)**	**i (kJ/kg air)**
1	**25**	**70**	13.898	60.555
2	32	62	18.64	79.92
3	**40**	**40**	18.64	88.246
4	**35**	58	20.668	88.246

The figures in bold are the design parameters that are determined by the environment.

The drying air and dryer design input values for secondary drying are shown in Table 9.

TABLE 9: Secondary drying air and dryer parameters

Parameter	**Value**	**Comment**	**Source**
Ambient Temperature (T_1)	25°C	Annual average	KenGen (2021e)
Relative Humidity (RH_1)	70%	Annual average	KenGen (2021e)
Ambient pressure (P_{amb})	101.5kPa		
Drying temperature (T_3)	50°C	Researched value	Njuguna (2021), Warangkana (2012)
Relative Humidity (RH_3)	30%	Researched value	Njuguna, (2021), Warangkana (2012)
ρ_{air} (@ T_3, RH_3 *and* P_{amb})	1.0791 kg/m^3		

The Mollier points for secondary drying are shown in Figure 17.

The corresponding air properties in the four sections of the dryer are as shown in Table 10.

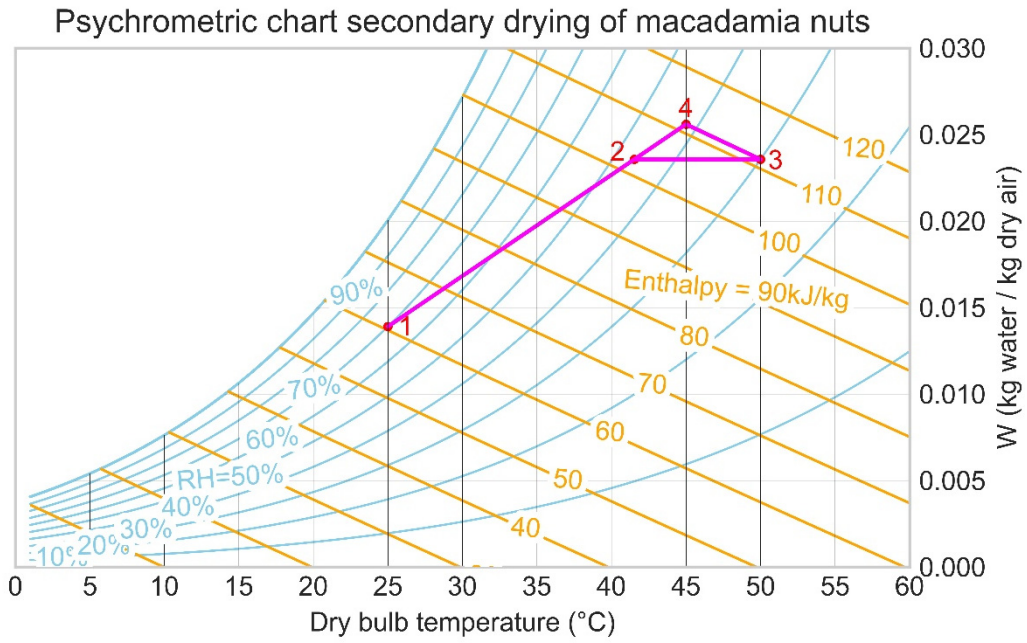

FIGURE 17: Data points plotted on Mollier chart for secondary drying

TABLE 10: Properties of each dryer section in the secondary drying phase at atmospheric pressure of 101.5 kPa

Point	**T (°C)**	**RH (%)**	**X (g water/kg air)**	**i (kJ/kg air)**
1	**25**	**70**	13.898	60.555
2	41.525	46.28	23.563	102.525
3	**50**	**30**	23.563	111.424
4	**45**	41.8	25.594	111.424

The figures in bold are the design parameters, that are determined by the environment.

4.6 Pilot plant cost estimate & financial modelling

For the pilot plant, the following factors need to be taken into consideration.

i. The location.
ii. Size of the plant.
iii. Financing considerations.
iv. Regulatory requirements.
v. Operation and maintenance.

4.6.1 The location

As location the site OW-803 has been proposed. Here, well conditions are favourable which allow maximum extraction of heat energy from the geothermal fluid without scaling inside the heat exchanger. The safety margin to allow for safe reinjection without scaling has been considered, too as well as proximity to other infrastructure like a power line, water supply, good road network and space availability. The site is also close to the two reinjection wells OW-801R1 and R2.

4.6.2 Size of the plant

For the pilot plant, a capacity of 20,000 kgs raw material per batch is being proposed. This has been derived from looking at the available transport axle limits in the republic of Kenya. For single axle trucks, a maximum of 10 tons is allowed, while for tandem axle, 18 tons is allowed (The Kenya Transporters Association, 2021). This capacity will allow for either one 18-ton truck or two 10-ton trucks to be processed at once.

For 20 tons of raw material with an average wet moisture content of 20%, the wet matter content is given as:

$$20\% \; x \; 20{,}000 \; kg \; = \; \mathbf{4{,}000 \; kg} \tag{13}$$

The dry matter content of the batch with 20% water content is:

$$(1 - \; 20\%) \; x \; 20{,}000 \; kg \; = \; \mathbf{16{,}000 \; kg} \tag{14}$$

At the final target dry basis moisture content of 1.5%, the total weight of the final product is:

$$\frac{16{,}000 \; kg}{(100 - 1.5)\%} \; = \; \frac{16{,}000}{0.985} \; = \; \mathbf{16{,}243.65 \; kg} \tag{15}$$

Hence, with the assumption that no solid material is lost during the drying process, the amount of water that must be carried away is thus:

$$20{,}000 - 16{,}243.65 \; = \; \mathbf{3{,}756.35 \; kg} \tag{16}$$

Silva et al. (2005) stated that the drying time for macadamia nuts using convectional hot air drying is about 144 hours. Njuguna (2021) reported that in Kenya, the drying process takes between 31-270 hours depending on the temperature used. Other factors that control time of drying include air speed and the starting moisture content of the raw material. For this pilot study, a period of 7 days is analysed assuming 24-hour running time daily. This gives a total drying period of 168 hours.

From the percentage of moisture evaporated in each drying phase, the time of drying for the two phases will be apportioned appropriately. Primary drying will take 53.7% of 168 hours, which is 90.216 hours, drying 2,017.16 kg of moisture in the process. Secondary drying will take 77.784 hours and carry away the balance of 1,739.19 kg of moisture in the process.

Using Equation 12, the amount of water to be carried away and Table 6, we can calculate the total mass flow of air required to carry away 2,017.16 kg of moisture in 90.216 hours:

$$G' = \frac{G}{t} = \frac{\frac{\Delta M}{\Delta X}}{t} = \frac{\frac{\Delta M}{t}}{\Delta X = (X_4 - X_3)} \quad G' = \frac{\frac{2{,}017.16\ kg}{90.216\ hours}}{(20.668 - 18.64)\frac{g_{water}}{kg_{air}}} \quad G' = 11{,}025.3\ kg\ air/hour \qquad (17)$$

The volume of air required for the primary process is then calculated from the density equation. The density of moist air at point (3) in the dryer in the primary drying process is used in the calculation:

$$V = \frac{G'_p}{\rho_{air\ at\ point\ T3}} = \frac{11{,}025.3\ kg/h}{1.1179\ kg/m^3} = \mathbf{9{,}862.4}\ \frac{\boldsymbol{m^3}}{\boldsymbol{h}} \qquad (18)$$

where G' = mass flow of air needed for the drying process (*kg/h*);
ΔM = difference in mass between the raw material and final product (*kg*);
t = drying time in hours (*h*);
ΔX = Change in the air water content between entry and exit of the dryer (*kg water/kg air*);
V = total volume of air needed for the drying process (m^3/h); and
$\rho_{air\ at\ point\ T3}$ = density of hot air inside the dryer (kg/m^3).

Similarly, the volumetric air flow rate per hour for secondary drying is calculated with the mass of water vapour to be carried away in 77.784 hours which is 1,739.19 kg. The water content of the air at points (3) and (4) are 23.563 g /kg and 25.594 g/kg, respectively, with the density of the air at point (3) being 1.0791 kg/m^3.

$$G'_s = 11{,}009\ kg\ air/hour \qquad (19)$$

And the volumetric flow rate for secondary drying is given by:

$$V = \frac{G'_s}{\rho_{air\ at\ point\ T3}} = \frac{11{,}009\ kg/h}{1.0791\ kg/m^3} = 10{,}202\ \frac{m^3}{h} \qquad (20)$$

The higher one of the two volumetric flow rates will be used for the design. A design factor of 20% will be incorporated in the design, hence, the design flow rate will be:

$$10{,}202\ {}^{m^3}/_{h} * 1.2 = 12{,}242.4\ \frac{m^3}{h} \qquad (21)$$

The time of drying is a function of dying temperature, relative humidity, air speed and raw material properties and placement on the drying bed. For the two drying stages, most of these other factors are fixed and the drying time can be controlled by varying the drying temperature and humidity in the dryer. Simulation of the two drying stages is shown in Figures 18 and 19. For this simulation, the difference in temperature of the incoming and outgoing air has been maintained at 5°C. Generally, at a constant temperature, increase in relative humidity means an increase in enthalpy. The moist air has a higher enthalpy and for the same difference in dryer inlet and outlet temperatures, it can carry more water vapor away. The relative humidity in the dryer however is limited by the relative humidity of the product to allow water to be carried away during the drying process.

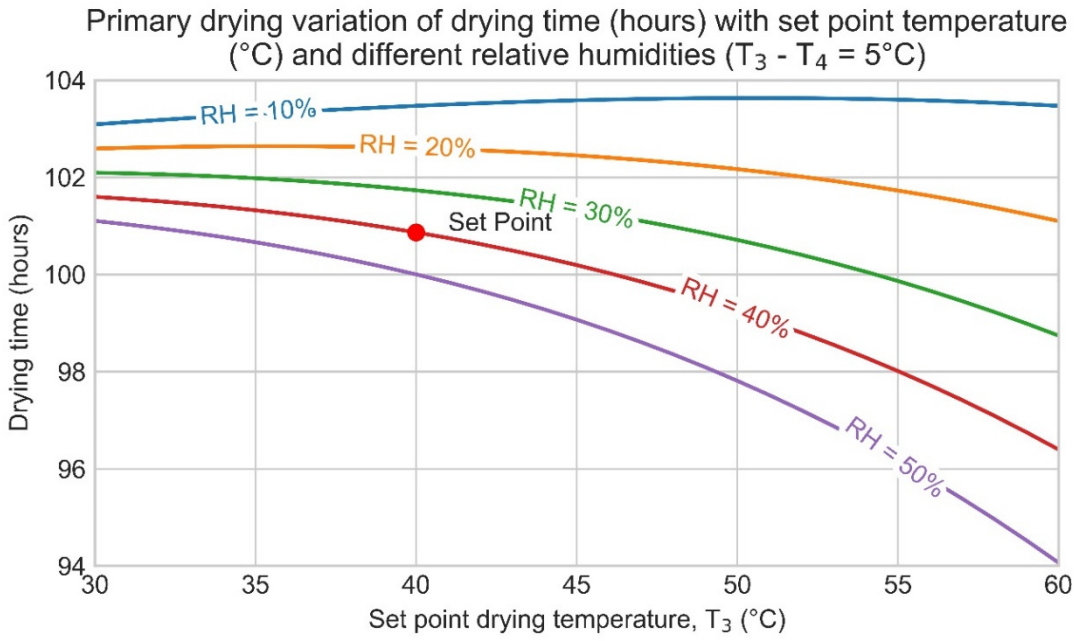

FIGURE 18: Primary phase variation of drying time with different temperatures and relative humidity values. (Homogenous wetness of raw product assumed, shape of macadamia nuts assumed to be perfect sphere with an equivalent diameter of 22.91mm)

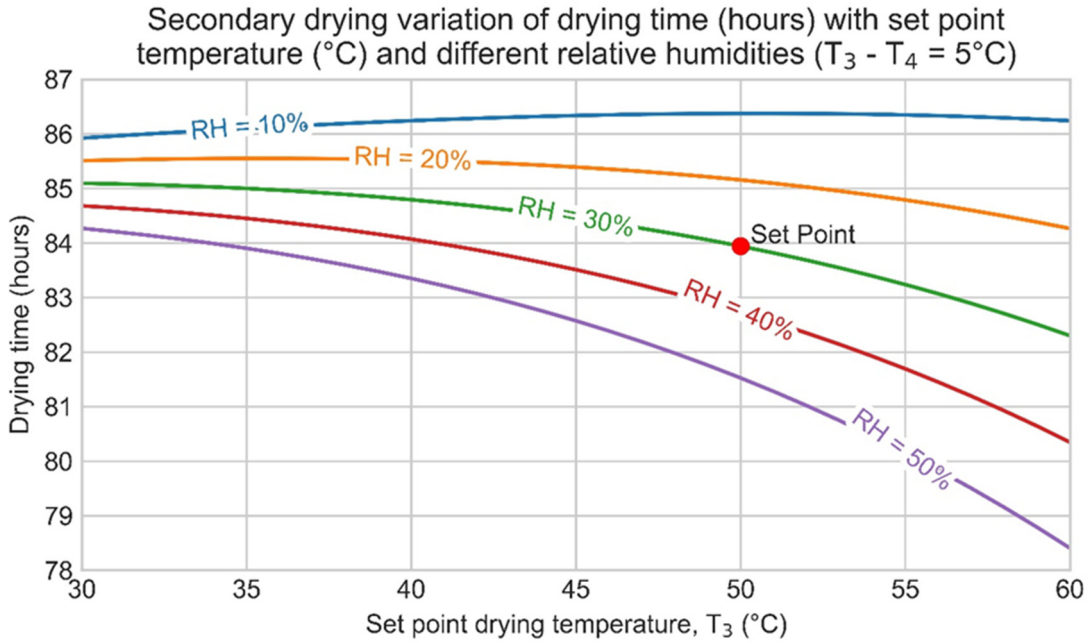

FIGURE 19: Secondary phase variation of drying time with different temperatures and relative humidity values. (Homogenous wetness of raw product assumed, shape of macadamia nuts assumed to be perfect sphere with an equivalent diameter of 22.91mm)

As shown in Figures 20 and 21, for both the primary and secondary drying phases, the difference in temperature of incoming and outgoing air has a high impact on the drying time. The bigger the difference

of these temperatures, the quicker the drying time. To prevent case hardening of the surface and deterioration of food quality, this difference is usually limited depending on the food material. It is also important to note that the conditions in this simulation might not be reachable in a practical application. The degree of saturation of air at point (4), e.g., always needs to be lower than in the atmosphere to allow for moisture being carried away.

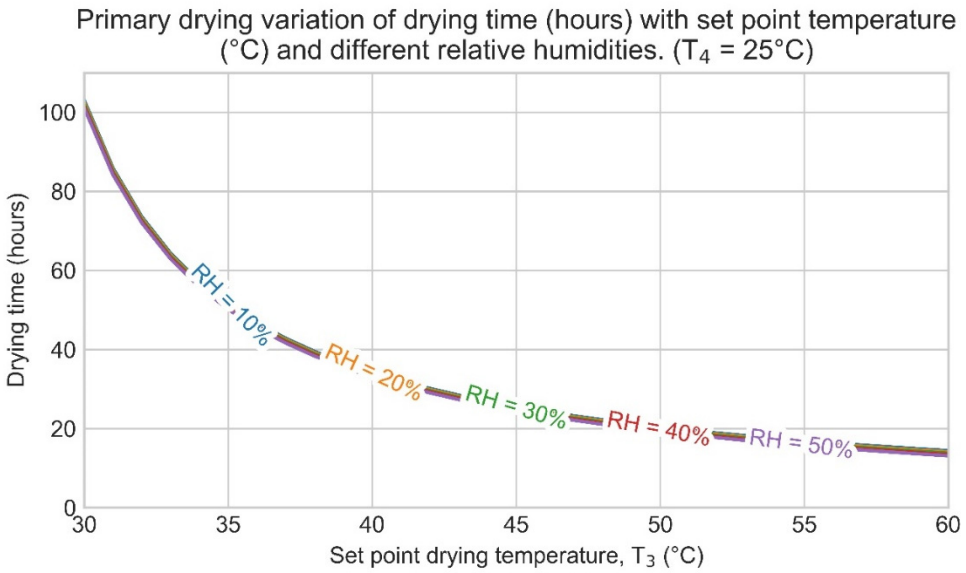

FIGURE 20: Primary phase variation of drying time with different temperatures and relative humidity values, with T_4 fixed at 25°C. (Homogenous wetness of raw product assumed, shape of macadamia nuts assumed to be perfect sphere with an equivalent diameter of 22.91mm)

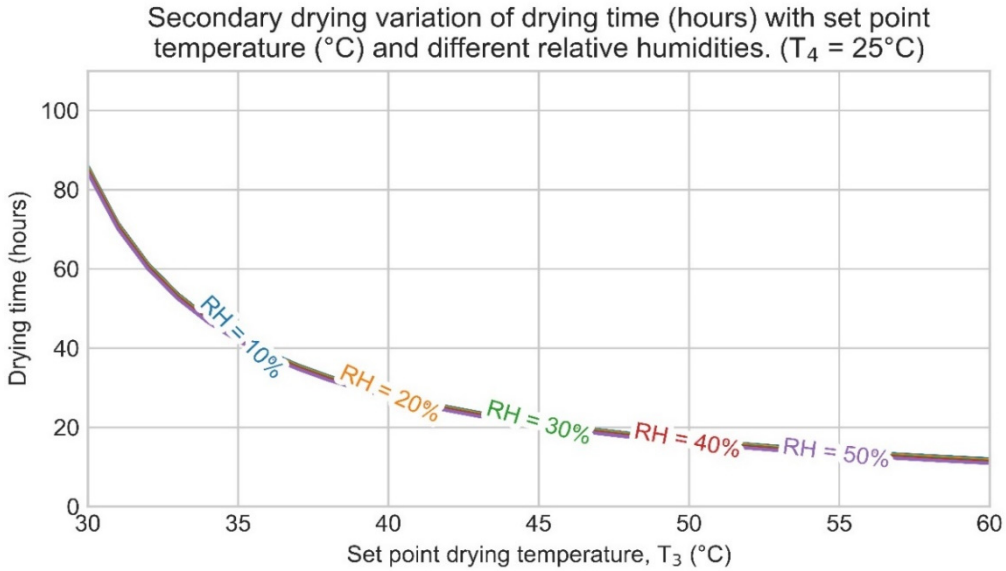

FIGURE 21: Secondary phase variation of drying time with different temperatures and relative humidity values, with T_4 fixed at 25°C. (Homogenous wetness of raw product assumed, shape of macadamia nuts assumed to be perfect sphere with an equivalent diameter of 22.91mm)

To estimate the volume of the shed required to dry 20 tons of fresh nuts the density needs to be known which varies with moisture content. For design purposes, a value of *689 kg/m³* will be used (MPD, 2021). A bed of base dimension 3.6 m x 3.6 m will be considered.

The area of the shed is given by:

$$area = 3.6\,m\ x\ 3.6\,m = 12.96\,m^2 \tag{22}$$

The volume occupied by 20 tons of fresh macadamia is given by:

$$volume = \frac{mass}{density} = \frac{20{,}000\ kg}{689\ \frac{kg}{m^3}} = 29.027\ m^3 \tag{23}$$

The height of the shed to hold the volume of macadamia nuts is given by:

$$height = \frac{volume}{area} = \frac{29.027\ m^3}{12.96\ m^2} = 2.24\,m \tag{24}$$

Using the initial assumption, that the macadamia nuts are spherical in shape and from the sphere packing density of around 74% (Wolfram, 2021), the void space or space available for air flow is calculated to be 26%.

$$volume_{void} = volume\ x\ 26\% = 29.027\ m^3\ x\ 0.26 = 7.54702\ m^3 \tag{25}$$

The cross-sectional area where the air flows through during the drying process can be approximated by dividing the void volume by the height of the bed.

$$area_{void} = volume_{void}\ /height = 7.54702\ m^3/2.24m = 3.369\ m^2 \tag{26}$$

The design volumetric flow rate per hour is converted to flow volume per second:

$$12{,}242.4\ {}^{m^3}/_{h} = \frac{12{,}242.4}{3{,}600}\ {}^{m^3}/_{s} = 3.4\ m^3/s \tag{27}$$

Linear air velocity per second, also known as the interstitial velocity V_I, can be calculated from the volumetric flow rate and the void area:

$$V_I = \frac{volumetric\ flow\ per\ second}{area_{void}} = \frac{3.4\ m^3/s}{3.369\ m^2} = 1.009\ m/s \tag{28}$$

A pressure drop is expected as the air moves up the bed. It is this pressure drop, in addition to the flow rate, that is used to size the air blower. The pressure drop in a packed bed is calculated using the Ergun equation:

$$f_p = \frac{150}{Re_p} + 1.75 \tag{29}$$

The friction factor f_p for the packed bed and the Reynolds number Re_p are defined as:

$$f_p = \frac{\Delta p}{L}\frac{D_p}{\rho {V_s}^2}\left(\frac{\varepsilon^3}{1-\varepsilon}\right) \qquad Re_p = \frac{D_p V_s \rho}{(1-\varepsilon)\mu} \tag{30}$$

where Δp = Pressure drop in the bed;
L = length of the bed;
D_p = Equivalent spherical diameter of the particle defined by $D_p = 6\ \frac{Volume\ of\ particle}{Surface\ area\ of\ particle}$
ρ = Density of the fluid;
μ = Dynamic viscosity of the fluid;
V_s = Superficial velocity ($V_s = \frac{Q}{A}$ where Q is the volumetric flow rate of the fluid and A is the cross-sectional area of the bed); and
ε = Void fraction of the bed.

Plugging the parameters for secondary drying in Equation 29 and if the average macadamia has a sphericity of 1 and an average diameter of 24.2 mm (Yangyuen and Laohavanich, 2018), we get a pressure drop of *785.13 N/m²* in the bed. This figure is multiplied by a factor of 1.25 for safety reasons.

$$\Delta p = 785.13\ x\ 1.25\ =\ \mathbf{982\ N/m^2} \quad (31)$$

Hence, the blower will need to overcome a pressure drop of about 1,000 N/m^2 inside the bed.

The heat requirement for the primary drying phase per hour is the heat required to change the conditions of the air at point (2) to those at point (3). This heat per hour, *Q'* is calculated as:

$$Q'_p\ =\ G'_p\ x\ (i_3 - i_2)\ =\ 11{,}026\ kg/h\ x\ (88.246 - 79.92)\ kJ/kg\ =\ \mathbf{91{,}802\ kJ/h} \quad (32)$$

The heat requirement for secondary drying is similarly calculated as:

$$Q'_s\ =\ G'_s\ x\ (i_3 - i_2)\ =\ 11{,}009\ kg/h\ x\ (111.424 - 102.525)\ kJ/kg\ =\ \mathbf{97{,}970\ kJ/h} \quad (33)$$

As secondary drying requires more power per hour, it will be the basis for the design. The power requirement in this phase is multiplied by a factor of 1.25 to account for energy losses in the equipment and the loss of loss to the environment as the dryer is not fully insulated.

$$Power\ required = Pw_r\ =\ Q'_s\ x\ 1.25\ =\ \mathbf{97{,}969.091\ kJ/h\ x\ 1.25\ =\ 122{,}462\ kJ/h} \quad (34)$$

This power will be supplied by geothermal water. The equation for calculating the amount of geothermal water needed to provide this energy is given below:

$$\boldsymbol{Q\ = m\ x\ c\ x\ \Delta T} \quad (35)$$

where Q = energy transferred in joules (J);
m = mass of the substance in kg;
c = specific heat capacity in J/kg degrees C; and
ΔT = temperature change in degrees C.

Equation 35 can be adapted to allow calculation of mass of water required per unit time if we know the power flow per unit time. The power required to warm the air will be extracted from heat supplied by geothermal water.

The proposed design has two stages of heating. This will prevent scaling and corrosion in the secondary loop which is the crimped spiral fin-and-tube heat exchanger (CSFTHX) that will warm the drying air. It will be supplied by clean water that has been preheated by the geothermal brine.

The geothermal brine, although chosen to avoid clogging and scaling, will be used in the primary heating loop to heat up clean potable water. The circuit of this water will be under a circulator pump and the

fluid will deliver the heat to the drying air via the spiral fin-and-tube heat exchanger. The primary circuit will have shell and tube heat exchangers. The shell and tube heat exchanger has been chosen as it has high temperature and pressure operating regimes, it is easy to clean and cost-effective

The approach temperature of the air to liquid heat exchanger is typically 8 to 14°C (Engineering Stack, 2021; Xchanger, 2021) and since the air will be heated by clean water in a secondary loop, we will maintain the temperature of this water below the boiling point at 90°C. The highest temperature required for the air is 50°C and using the typical approach temperature of 14°C, the exit temperature of the secondary circuit is 64°C. The ΔT for this circuit is therefore 26°C.

Hence, by using the specific heat capacity of water which is 4.182kJ/kg, the mass flow rate required to warm the air going into the dryer is:

$$\dot{Q} = \dot{m}\ x\ c\ x\ \Delta T \quad 122{,}462\ kJ/h = \dot{m}\ x\ 4.182\ kJ/kg\ x\ 26°C \qquad \dot{m} = 1{,}127\ kg/h \qquad (36)$$

Hence, the circulator pump should be able to move about 1.13 m^3 of 90°C hot circulation fluid every hour. The circulation fluid will be heated by the geothermal fluid. An overall efficiency of 90% of the two heat exchangers including heat losses in the pipes will be assumed. Hence, the actual heat to be supplied by the geothermal fluid is:

$$\dot{Q}_{geo\_fluid} = \frac{122{,}462}{90\%}\frac{kJ}{h} = 136{,}067\ kJ/h \qquad (37)$$

As earlier discussed, the maximum tolerable temperature drop in the geothermal fluid that will reduce scaling in the heat exchangers is determined by the wellhead pressure. While discharging through a 5" lip pipe, the wellhead pressure was 6.1 bar, and the steam and water mass flow rates were 15.8 t/hr (18.2% of total mass flow) and 70.7 t/hr (81.8% of total mass flow), respectively. At a wellhead pressure of 6.1 bar (a), the temperature of the saturated steam is 159.48°C. Heating of the circulation fluid in the dryer will be done by both the water and the steam contained in the well discharge. As the fluid is cooled in the heat exchanger, some of the steam will condense into liquid and lose its internal energy. An estimate of the required mass flow is calculated from the heat obtained by condensation of steam and the heat obtained by cooling of the fluid:

$$\dot{Q}_{geo\_fluid} = \dot{m}_w\ x\ c_w\ x\ \Delta T + \dot{m}_{s\_cond}\ x\ \Delta H_{cond} + \dot{m}_{s\_cool}\ x\ \Delta H_{cool} \qquad (38)$$

where $\dot{Q}_{geo\_fluid}$ = energy to be derived from the geothermal fluid per hour (kJ/h);
$\dot{m}_w$ = mass of the water phase (kg/h);
c_w = specific heat capacity in kJ/kg degrees C;
ΔT = temperature change in degrees C;
ΔH_{s_cond} = change in the specific enthalpy of the steam due to condensation;
ΔH_{s_cool} = change in the specific enthalpy of the steam due to cooling;
$\dot{m}_{s\_cond}$ = mass of steam that is condensing (steam to brine phase change); and
$\dot{m}_{s\_cool}$ = mass of steam that is cooling (steam at 159.48°C to steam at 120°C).

The change in enthalpy in the steam phase as it condenses from 159.48°C to water at 120°C is calculated below:

$$\overline{\Delta H}_{s\_cond} = H^{159.48} - h^{120} \qquad \overline{\Delta H}_{s\_cond} = 2{,}756.86 - 503.785 = 2{,}253.075\ kJ/kg \qquad (39)$$

where $H^{159.48}$ = specific enthalpy of steam at 159.48°C; and
h^{120} = specific enthalpy of water at 120°C.

The change in enthalpy in the steam phase as it cools from 159.48°C to steam at 120°C is calculated below:

$$\overline{\Delta H}_{s\_cool} = H^{159.48} - H^{120} \qquad \overline{\Delta H}_{s\_cool} = 2{,}756.86 - 2{,}705.93 = 50.93\ kJ/kg \tag{40}$$

where $H^{159.48}$ = specific enthalpy of steam at 159.48°C; and
H^{120} = specific enthalpy of steam at 120°C.

From practical observations we know that about 15% of the steam will be condensed during cooling (Sigurjón Arason, Chief Engineer, R&D Division at Matis, personal communication, 29 October 2021). Hence, the actual changes in enthalpies ΔH_{s_cool} and ΔH_{s_cond} are:

$$\Delta H_{s\_cond} = 15\%\ x\ 2{,}253.075 = 337.961\ kJ/kg \tag{41}$$

$$\Delta H_{s\_cool} = 85\%\ x\ 50.93 kJ/kg = 43.29\ kJ/kg \tag{42}$$

Equation 38 can be written in terms of steam composition assuming that 18.2% of the fluid is in form of steam:

$$\dot{\boldsymbol{Q}}_{\boldsymbol{geo\_fluid}} = \dot{m}_w\ x\ c_w\ x\ \Delta T + \dot{m}_s\ x\ \Delta H_s$$

$$= 4.47\ \boldsymbol{x}\ \dot{m}_s\ \boldsymbol{x} 4.184 kJ/kg\ \boldsymbol{x}\ 39.48°C + 0.15 m_s\ \boldsymbol{x} 337.9 kJ/kg + 0.85 m_s\ x\ 43.3\ kJ/kg \tag{43}$$

Solving equations 38 and 43 gives a steam flow rate of 164.76 kg/h and the water flow is therefore 737.24 kg/h. The total expected geothermal flow is therefore 902 kg/h. This represents 0.95% of the total flow available from OW-803A, showing a great potential for upscaling of the operations after successful tests of the dryer.

Table 11 show that within the peak harvesting period of 16 to 20 weeks, it is possible to dry more than 50% of the expected production from Kenya with the geothermal fluid from just one well in Olkaria (OW-803A).

TABLE 11: Potential of fully utilizing the fluids from OW-803A for macadamia drying

Well flow rate (kg/hr)	Tons dried	Comments
902	20	Tons of macadamia dried in one week in the pilot plant
94,700	2,100	Potential tons of macadamia dried by fluid from this well in one week
	2,100 x 16 = 33,600	Potential tons of macadamia dried by fluid from this well in 16 weeks
33,600 tons is slightly above the 50% projected nut in shell production in Kenya by the year 2022 (Quiroz et al., 2019).		

Figure 22 shows the CO_2 emissions that can be avoided if all the expected annual production of 60,000 metric tons in Kenya was dried using geothermal fluids instead of biomass or fossil fuels as it is the case today.

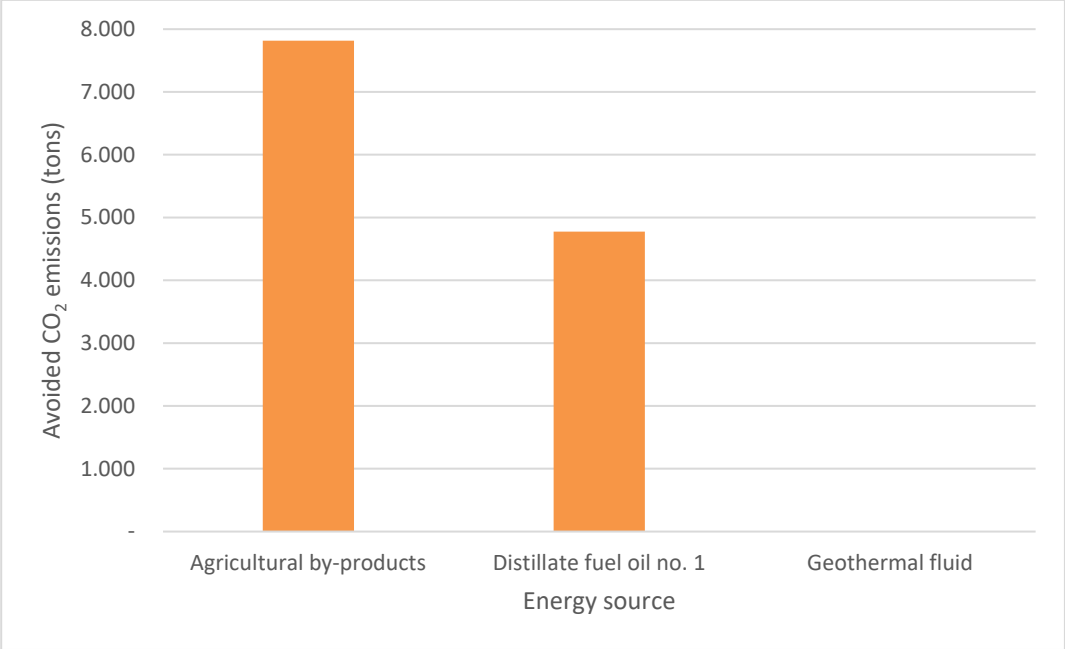

FIGURE 22: Avoided equivalent CO_2 emissions if geothermal fluids were used in drying of 60,000 metric tons of macadamia in Kenya

4.6.3 Stakeholders engagement

The following stakeholders and government institutions will need to be consulted for buy-in of the design, before commencement of the project:

Kenya Wildlife Service (KWS) – This is a state corporation tasked with conservation and management of wildlife in Kenya. As the Olkaria field is inside a Hells Gate National Park, KWS is a key stakeholder to consult on the planned implementation.

Kenya Bureau of Standards (KEBS) – This is a government agency that deals with standards, metrology, and conformity assessment. As the macadamia nut requires to be produced in a certain quality, KEBS will be a stakeholder to ensure conformance to international standards.

Macadamia Nut Processors - These companies are potential customers and they need to learn about the option to uset geothermal instead of fossil fuels, which are contributing to global warming.

National Environmental Management Authority (NEMA) – This agency evaluates impacts of various developments on the environment. Since this project is sustainable and reduced emissions, it is expected to be encouraged. Aspects that could have a negative impact will be mitigated.

Local community – The local communities around any development project are key stakeholders as they interact with the project every day. The generation of new jobs for local community members is a positive outcome anticipated in this project.

Farmers – It will be necessary to engage macadamia farmers as they will be the source of the raw product.

4.6.4 Financial considerations

As KenGen Plc continues its diversification process, venturing into post-harvest loss prevention is a worthy cause. Estimates put cereal post-harvest losses in many African countries at around 25% while horticultural crops and roots losses can reach 50% (UNEP, 2021). Either through KenGen B or KESEL, the company can pursue partnerships with private sector partners to venture into this industry.

The low-pressure geothermal wells are a resource that has the potential to contribute to Kenya's Big 4 Action plan, as food security and nutrition is one of the key pillars of the agenda. Geothermal energy is a green energy source and it will be possible to attract different international partners to collaborate on future expansion. There is a premium tied to products produced in a sustainable manner which makes the investment to process the food by use of geothermal energy lucrative.

The estimated costs for building the pilot plant as designed here is shown in Table 12.

TABLE 12: Estimated Cost of a Macadamia Dryer Pilot Plant

No	**Description**	**Estimated Cost (KES)**
1	Mechanical Fabrication	850,000
2	Electrical Components	650,000
3	Heat Exchangers	660,000
4	Control System	500,000
5	Sensors	520,000
6	Fabrication Costs	560,000
7	Steam line connection	3,000,000
Total		**6,740,000**

The income stream has been estimated as shown in Table 13. It has been assumed that the dryer will be used at a capacity factor of 100% for a total of 20 weeks during the peak harvesting time. A capacity factor of 50% has been assumed during the rest of the year where the dryer can be used for drying different products.

TABLE 13: Estimated Annual Income and O & M costs

Description	**Amount (KES)**	**Unit**	**Quantity**	**Subtotal (KES)**
Capital Cost	(6,740,000)	Au	1	(6,740,000)
Weekly Expenditure (Peak)	81,088	Week	20	1,621,769
Weekly Earnings (Peak)	158,277.78	Week	20	3,165,556
Weekly Expenditure (Off-Peak)	40,544	Week	32	1,297,415
Weekly Earnings (Off-Peak)	79,138.89	Week	32	2,532,444
Maintenance	3,888	Au	52	202,200
Total Income per year				**5,698,000**
Total Expenditure per year				**3,121,385**
Net income per year				**2,576,615**
Capital Expenditure				**(6,740,000)**

The discounted payback period was calculated using the present cashflow with a discount rate of 15%. Table 14 shows the results of the discounted payback calculations and Figure 23 shows the payback period to be around 3.6 years.

TABLE 14: Discounted Payback Period with r=15%

Description	Cash Flow	PV Cash Flow	Discounted Balance
Capital Expenditure	-KES 6,740,000.00	-KES 6,740,000.00	-KES 6,740,000.00
Net income year 1	KES 2,576,615.38	KES 2,240,535.12	-KES 4,499,464.88
Net income year 2	KES 2,576,615.38	KES 1,948,291.41	-KES 2,551,173.48
Net income year 3	KES 2,576,615.38	KES 1,694,166.44	-KES 857,007.04
Net income year 4	KES 2,576,615.38	KES 1,473,188.21	KES 616,181.17
Net income year 5	KES 2,576,615.38	KES 1,281,033.23	KES 1,897,214.40
Net income year 6	KES 2,576,615.38	KES 1,113,941.93	KES 3,011,156.33
Net income year 7	KES 2,576,615.38	KES 968,645.16	KES 3,979,801.49
Net income year 8	KES 2,576,615.38	KES 842,300.14	KES 4,822,101.63
Net income year 9	KES 2,576,615.38	KES 732,434.90	KES 5,554,536.54
Net income year 10	KES 2,576,615.38	KES 636,899.92	KES 6,191,436.45
Net income year 11	KES 2,576,615.38	KES 553,826.01	KES 6,745,262.47
Net income year 12	KES 2,576,615.38	KES 481,587.84	KES 7,226,850.31

FIGURE 23: Discounted payback period with r=15%

4.6.5 Operation and maintenance

As the pilot plant will be constructed locally and only parts not available in Kenya will be imported, the following ingenuity options will be incorporated in the design for ease of operation and maintenance:

Automation: Prudent control of the dryer parameters including relative humidity, temperature, and air speed is critical for determining the quality of the final product. These parameters will best be monitored

by an autonomous system and changed as needed. A PLC or microcontroller-based system will be adapted for the pilot system.

Modular design: The dryer design has been sub-divided into smaller components to allow for independent modification, replacement, and exchange with similar parts without affecting the whole system.

Redundancy: Critical components will be duplicated to increase the overall efficiency of the system by reducing outage due to breakdown.

Adoption to other products: As the peak harvesting period of macadamia nuts is only 4 to 5 months, the dryer will be constructed to allow for easy adaptation to dry other products that are locally available. This will reduce post-harvest losses and allows for access of proper nutrition throughout the year.

Operations: As most of the parts will be locally sourced and all fabrication and assembly will be done locally, operators will be thoroughly trained to ensure efficient and safe operations of the dryer.

5. CONCLUSION & RECOMMENDATIONS

5.1 Conclusions

Following the recommendations of different authors including Toyoda et al. (1991), Wang et al. (2013), Phusampao (2014), Tumba (2018), Ertekin and Firat (2017), and Njuguna (2021), a two-stage process to dry macadamia nuts to attain the best quality has been designed. The primary stage will take the moisture content from 25% to 12% d.b. in 90.2 hours and dry 53.7% of the moisture, while during the secondary stage the final moisture content will drop to 1.5% in 77.8 hours, eliminating 46.3% of the moisture.

Primary drying will be carried out at a temperature of 40°C and relative humidity of 40%, while secondary drying will be done at 50°C and relative humidity of 30%.

The macadamia dryer designed here has the potential to positively impact the following stakeholders and sectors in both the local and the wider Kenyan economy:

KenGen – The company will benefit from a new revenue stream by utilizing low pressure wells that have been capped after drilling was completed.

Environment – Drying by use of geothermal energy will help to reduce greenhouse gases emitted by the currently in use biomass or fossil fuel fired dryers.

Farmers – Many farmers incur losses due to lack of access to affordable and reliable drying facilities. A geothermal powered dryer is guaranteed to have a high availability and the costs will be lower as the ‘fuel’ used is literally ‘free’.

Jobs – New jobs are expected to be created if drying of not only macadamia, but other agricultural produce as well becomes embraced in Kenya.

Customers – Macadamia consumers will be able to enjoy a product that is produced at optimal conditions and derive more benefits from the product.

Traders – Traders who are currently exorbitantly charged by fossil fired dryer operators will benefit from the lower costs when geothermal energy is used for drying.

Food Security – Kenya has seasons of excess food production and seasons of low food production. As the country is geographically vast, some areas may have an excess of a certain produce that cannot be transported to another area due to perishability of the produce. If the society accepts drying as a food preservation method, this has the potential to change the food security in the country.

5.2 Recommendations

1. It is recommended that KenGen seeks relevant approvals and partnerships to implement this proposal which has the ability to improve the quality of life for many Kenyans and will also be a new revenue stream for the company.

2. As the wells self-discharge, flashing of the geothermal fluid produces steam. This pilot project is designed to utilize the hot brine. The steam produced can be used for other purposes, including powering of a steam engine to produce power to run other equipment like fans for driving the air, reinjection pumps or semi-automated nut cracking machines. The possibility to use the steam as a source of heat for roasting macadamia nuts should be studied further.

3. As macadamia nuts have a peak harvesting season, the pilot dryers should be designed in such a way that they can be adapted to dry other farm produce when no nuts are harvested. This will allow for optimization of the dryer use and improve the capacity factor.

4. To improve the final product quality, the pilot design should incorporate reversible air flow to reduce the moisture gradient normally experienced in static batch dryers.

ACKNOWLEDGEMENTS

I would like to appreciate my employer KenGen and the people of Iceland for giving me the opportunity to do this project. Hats off to my supervisor Sigurjón Arason for giving me good advice, providing guidance, comments and corrections during my project and report.

My sincere thanks to the GRÓ GTP team for assistance granted to me at different stages of the programme. I am grateful to the director Mr Guðni Axelsson, deputy director Mr Ingimar G. Haraldsson, Ms Málfríður Ómarsdóttir, Ms Vigdís Harðardóttir and Mr Markús A. G. Wilde for the different roles they have played to make my stay in Iceland memorable.

To Páll Valdimarsson and María Sigríður Guðjónsdóttir, thank you for making Utilization specialization impactful to my career. To all my GRÓ GTP fellows, thank you for the great moments during the last six months.

Special thanks to my family, especially to my dad for constant follow-up, my wife Ann and children Jayden and Salma for the encouragement and for granting me the peace to pursue this, away from home. To my siblings Lillian, Lena and Kevin, thank you for your constant support in all ways that I needed you during this period.

I am grateful to God for providing me with good health, strength, and peace of mind during my entire stay in Iceland.

REFERENCES

Andrade, R.D.P., Lemus, R.M., and Perez, C.E.C., 2011: Models of sorption isotherms for food: uses and limitations. *revista de la facultad de quõmica farmaceutica, Universidad de Antioquia, 18(3),* 325-334.

Arason, S., 2018: Utilization of geothermal energy for drying fish/food products and new drying technologies in Iceland. *Paper presented at the International Geothermal Conference IGC 2018*, Reykjavík, 7 pp.

Arason, S., 2021: *Geothermal training in Iceland 2021 Heating and drying*. GRÓ GTP, Iceland, unpublished lectures, 179 pp.

Axelsson, G., 2013: Geothermal well testing. *Presented at "Short Course V on Conceptual Modelling of Geothermal System", organized by UNU-GTP and LaGeo, Santa Tecla, El Salvador,* 30 pp.

Bloomquist, R.G., 2006: Economic Benefits of Mineral Extraction from Geothermal Brines. *Washington State University Extension Energy Program, 2006*.

Britannica, 2021: *Britannica,* website: *https://www.britannica.com/science/geothermal-energy/*

Dickson, M.H., and Fanelli M., 2004: *What is geothermal energy?* Instituto di Geoscienze e Georisorse, CNR, Pisa, Italy, report, 61 pp.

Engineering Stack, 2021: *Engineering Stack,* website: *https://www.engstack.com/blog/air-cooled-heat-exchangers-design-good-practices/*

Ertekin, C., and Firat, M.Z., 2017: A comprehensive review of thin layer drying models used in agricultural products. *Critical Reviews in Food Science and Nutrition*, *57(4),* 701-717.

Gao, X., Wang, J., and Horne, R.N., 2020: Downhole measurement of enthalpy in geothermal wells – An analytical, experimental and numerical study. *Geothermics, 88,* 101902.

Gehringer, M., and Loksha V., 2012: *Geothermal handbook: planning and financing power generation*. The World Bank, Energy Sector Management Assistance Program, Washington DC, Technical Report 002/12, 150 pp.

Gunnlaugsson, E., Ármannsson, H., Thorhallsson, S., and Steingrímsson, B., 2014: Problems in geothermal operation – scaling and corrosion. *Presented at "Short Course VI on Utilization of Low- and Medium-Enthalpy Geothermal Resources and Financial Aspects of Utilization", organized by UNU-GTP and LaGeo, Santa Tecla, El Salvador,* 18 pp.

INC, 2018.: *International nut and dried fruit council,* Macadamia Technical Information, report, 15pp.

Ingason, K., 2021: *Well design and geothermal drilling technology*. GRÓ GTP, Iceland, unpublished lectures, 150 pp.

KenGen, 2021a: *Geothermal generation summary for 27th September 2021.* Kenya Electricity Generating Company Plc, unpublished report.

KenGen, 2021b: *Olkaria SEP Discharge data.* Kenya Electricity Generating Company Plc, unpublished report.

KenGen, 2021c: *A Drawing of sectors in Olkaria Geothermal Field.* Kenya Electricity Generating Company Plc, unpublished report.

KenGen, 2021d: *Silica scaling assessment OW803A.* Kenya Electricity Generating Company Plc, unpublished report.

KenGen, 2021e: *Environmental Meteorology and Air Quality Report – September 2021.* Kenya Electricity Generating Company Plc, unpublished report.

Kenya Power, 2021: The Kenya Power and Lighting Company Plc, *Annual Report and Financial Statements 2019/2020.* 164 pp

KNBS (Kenya National Bureau of Statistics), 2019: *2019 Kenya Population and Housing Census*: Volume I: Population by County and Sub-County, November 2019, 49 pp.

Mangi, P.M., 2019: Geothermal exploration in Kenya – Status report and updates. *Paper Presented at SDG Short Course IV on Exploration and Development of Geothermal Resources, organized by UNU-GTP and KenGen, at Lake Bogoria and Lake Naivasha, Kenya, Nov. 13 – Dec. 3, 2019*, 25 pp.

Mason, R. L., and Wills, R.B.H., 2000: Macadamia nut quality research: The processing challenge. *Food Australia,* 52(9), 416–419. In Silva, F.A., Marsaioli, A.Jr., Maximo, G.J., Silva, M.A.A.P, and Goncalves, L.A.G., 2005: Microwave assisted drying of macadamia nuts. *Journal of Food Engineering, 77,* 550–558.

Maxim International, 2019: *Maxim,* website: *https://www.maxim.com/food-drink/macadamia-nuts-superfood-diet-2019-12/*

MPD, 2021: *Machine Process and Design*, website: *http://www.mpd-inc.com/bulk-density/*

Mujumdar, A.S., and Law, C.L., 2010: Drying technology: Trends and applications in postharvest technology. *Food and Bioprocess Technology, 3(6),* 843–852.

Mujumdar, A.S., and Wu, Z.H., 2010. Thermal drying technologies: New developments and future R & D potential. In: Jangam, S.V., and Thorat, B.N. (eds.), *R&D needs, challenges and opportunities for innovation in drying technology*. e-book, 65-86. Available at: https://arunmujumdar.com/wp-content/uploads/2020/03/e-book-on-RD-opportunities-in-drying.pdf

Mwangi, M., and Mburu, M., 2005: Update of geothermal development in Kenya and other African countries. In Mwangi, M. (lecturer): *Lectures on geothermal in Kenya and Africa*. UNU-GTP, Iceland, report 4, 1-13.

Njuguna, E.N, 2019: Utilization of brine from Well 07 in the Menengai geothermal field for a geothermal spa. Report 21 in: *Geothermal Training in Iceland 2019.* UNU-GTP, Iceland, 447-476.

Njuguna, S.N., 2021: *evaluating effects of drying method using colour image analysis on quality of macadamia nuts*. Master Thesis, Jomo Kenyatta University of Agriculture and Technology, Kenya.

Omenda, P., Mangi, P., Ofwona, C., and Mwangi, M., 2020: Country update report for Kenya 2015-2019. *Proceedings of the World Geothermal Congress 2020+1,* Reykjavík, Iceland, 16 pp.

Phusampao, C., 2014: *Drying of macadamia nuts*. Ph.D. Thesis, Graduate School, Silpakorn University, Thailand.

PDU, 2021: *The President's Delivery Unit*, website: *https://big4.delivery.go.ke/*

Quiroz, D., Kuepper, B., Wachira, J., and Emmott, A., 2019: *Value Chain Analysis of Macadamia Nuts in Kenya,* research commissioned by CBI, Amsterdam, the Netherlands: Profundo, 98 pp.

IRRI, 2021: *Rice Knowledge Bank,* website: *http://www.knowledgebank.irri.org/step-by-step-production/postharvest/drying/mechanical-drying-systems/examples-of-mechanical-dryers/item/fixed-bed-batch-dryer*

Sabarez, H.T., 2018: Thermal drying of foods. In: Rosenthal, A., Deliza, R., Chanes, J.W., and Canovas, G.V.B., (eds), *Fruit Preservation Novel and Convectional Technologies.* Springer, NY, 181–210.

Silva, F.A., Marsaioli, A.Jr., Maximo, G.J., Silva, M.A.A.P, and Goncalves, L.A.G., 2005: Microwave assisted drying of macadamia nuts. *Journal of Food Engineering, 77,* 550–558.

Tumba, K., 2018: Convective air-drying characteristics of ground macadamia nuts. *Scientific Study and Research: Chemistry and Chemical Engineering, 19(3),* 243-255.

Tesha, 2006: Utilization of brine water for copra drying in Lahendong geothermal field, Indonesia. Report 20 in: *Geothermal Training in Iceland 2006*. UNU-GTP, Iceland, 453-470.

The Kenya Transporters Association, 2021: *The Kenya Transporters Association*, website: *https://www.kta.co.ke/index.php/2015-05-22-13-26-39/twr-axleloadlimits?showall=1&limitstart=*

ThinkGeoEnergy, 2021: *What is Geothermal Energy?,* website: *https://www.thinkgeoenergy.com/geothermal/what-is-geothermal-energy./*

Tompson, G.H.J., Verreault, D., and Tompson, H.B., 2009: Hawaii macadamia nut company. *The Journal of Entrepreneurial Finance, 13(2),* 103-118.

Toyoda, K., Shibata, Y., Mwangi, G.G., Takeuchi, R., and Kojima, H., 1991: Study on drying characteristics of macadamia nuts. *Japan. J. Trop. Agr. 35(2):* 92-97.

UNEP, 2021: *UNEP,* website: *https://www.unep.org/thinkeatsave/get-informed/worldwide-food-waste*

USAID, 2021: *USAID*, website: *https://www.usaid.gov/kenya/agriculture-and-food-security*

Wang, Y., Zhang, L., Johnson, J., Gao, M., Tang, J., Powers, J.R., and Wang, S., 2013: Developing hot air-assisted radio frequency drying for in-shell macadamia nuts. *Food Bioprocess Technol,7,* 278–288.

Warangkana, S., 2012: *Effects of Postharvest Treatments on Macadamia Nut Quality*. Ph.D. Thesis, School of Chemical Engineering, The University of New South Wales, Australia.

Wolfram, 2021: *Wolfram Math World*, website: *https://mathworld.wolfram.com/SpherePacking.html*

Xchanger, 2021: *Xchanger Inc*, website: *https://xchanger.com/faq/*

Yangyuen, S., and Laohavanich, J., 2018: Development of a semi-automatic macadamia cracking machine. *Engineering and Applied Science Research, 45(4),* 256-261.

Zuza, E.J., Maseyk, K., Bhagwat, S., Emmott, A., Rawes, W., and Araya, Y.N., 2021: Review of macadamia production in Malawi: Focusing on what, where, how much is produced and major constraints. *Agriculture, 11(2),* 152.